Light-Driven Bimorphic Soft Actuators: Design, Fabrication and Properties

Abstract: Soft robotics that can move like living organisms and adapt to their surroundings are currently in the limelight from fundenmental research to technological applications due to advantageous characteristics of superior flexibility and adaptability as well as human-friendly interaction compared with conventional rigid robotics. Light-fulled soft actuators could be one of most promising candidates to promote the future development of untethered soft robotics with bioinspired intelligence. Herein, we provide a state-of-the-art review on recent advances of light-driven bimorphic soft actuators that combine a photoactive layer with a passive layer in one single bilayered system, which could endow soft actuators with unprecedented features such as ultrasensitivity, programmability, superior compatibility, robust functionality and easy controllability. We begin with a overview on the working mechanism of bimorphic soft actuators and promising synthetic strategies towards light-driven soft robotics or machines. Then bimorphic soft actuators based on photothermal and photochemical effects are sequentially introduced with an emphasis on the design strategy, fundamental performance, underlying mechanism as well as emerging applications. Finally, this review is concluded with a perspective on the exisiting challenges and future opportunities in the rising area of bioinspired intelligent soft robotics which embrace interdisciplinary area including biology, physics, chemistry, engineering, materials science, nanoscience and nanotechnology.

Keywords: Soft robotics, bimorphic soft actuators, light-driven, bioinspired

1. Introduction

Soft actuation is ubiquitous in living organisms ranging from terrestrial worms to sea animals, starfish and octopuses, where highly flexible and deformable soft bodies allow their access to small apertures to shelter or prey, and help adapt to unpredictable and ever-changing environments.[1,2] Over 650 named skeletal muscles can be found in the body of adult mammals or human beings, which are known to make up approximately 40% of the total body mass and play a significant role in performing a variety of complex movements and vital functions. Taking inspiration from natural creatures,

researchers have recently devoted extensive efforts to developing programmable and reconfigurable soft actuators towards next-generation soft robotics with bioinspired intelligence.[3-5] Compared with conventional rigid robotics that have become matured technologies from industrial arms on production lines to autonomous drones, semiautonomous vacuum cleaners and driverless vehicles, bioinspired soft robotics built with soft materials focuses on compliance and deformability in the interaction with the environment, and could exhibit unprecedented characteristics of superior flexibility and adaptability as well as "human-friendly" working manner, which is expected to enable robust and customizable soft machines that can perform various complicated tasks and intelligently adapt to ever-changing complex environments.[2,6,7]

Soft actuators are generally defined as highly deformable materials or nanocomposites that can convert various forms of external stimulations or input energy into desired forces/torques and mechanical motions. A wide range of soft materials such as gels,[8,9] elastomers,[10] liquid crystals,[11,12] flexible sheets[13] have been used to construct advanced functional soft actuators that could be powered by different methods such as light,[14,15] electric,[16] magnetic,[17] humidity,[18] pneumatic or hydraulic,[19,20] combustion,[21] and biohybrid actuation.[22] Among these, vacuum-powered soft pneumatic actuators have been commercialized and widely used in mobile robots, assistive wearable devices, and many other rehabilitative technologies although there is a major limitation of needing a tethered connection to the external pump. Light-driven soft actuators that exhibit superior optical-to-mechanical energy conversion capacity have recently attracted increasingly research attentions thanks to their remarkablefeatures of remote, spatial and temporal controllability.[23,24] As one of most versatile, inexhaustible and sustainable energy source, light is ubiquitous in our dailylife, more than 50% of solar radiations arrives at the earth in the form of near-infrared light, and its physical parameters including intensity, wavelength, and polarization can be facilely tailored with high spatial and temporal resolution, and on-demand controlled through laboratory-level mirror scanners and digital micromirrors as well as commercially available computer projectors.[6,25] All these outstanding advantages make it possible to

simplify the complex nanoarchitectures of conventional soft actuators towards the development of untethered sunlight-fuelled soft robotics with bioinspired intelligence.

Up to now, light-driven soft actuators with different structures has been presented including homogenous structure,[26] gradient structure,[27] bimorph structure.[28] For soft actuators with homogenous structure, non-homogenous light irradiations are often utilized to obtain a dynamic stress gradient along the thickness of actuators. For soft actuators with gradient structure, the materials gradient within a monolayer actuator is prefabricated to generate a static stress gradient along its thickness, which could result in the reversible shape deformation of soft actuators upon external light irradiations. Soft actuators with homogenous and gradient structures have obvious advantages in terms of simple materials components and superior structural stability, but they face some grand challenges related to difficulties in improving sensitivity, enriching programable deformation and endowing with functionalization. By comparison, photoactive soft actuators with bimorph structure, i.e., light-driven bimorphic soft actuators, combine a photoactive layer with a passive layer in one single bilayered system, where the large mismatch between both layers replace the continuous gradient in response to external light activation could endow soft actuators with unprecedented features such as ultrasensitivity, programmability, superior compatibility, robust functionality and easy controllability.[29] Besides abundance in selection of photoactive and passive materials with diverse shapes,[30-33] the physical parameters of soft materials such as Young's modulus and coefficient of thermal expansion (CTE) of different layers could be easily customized on-demand, for example, the anisotropy of bimorphic soft actuators could be facilely achieved by introducing anisotropic nanomaterials into appropriate layers,[34] and sophisticated control over the anisotropy direction could generate a wide variety of shape deformations and bioinspired motions such as bending, spiral, twisting, and oscillation. Furthermore, both surface wrinkling and shape deformation of soft actuators could be programmed through talioring different layer thicknesses and induced strain between layers.[35] Therefore, light-driven bimorphic soft

actuators is expected to opened up numerous exciting possibilities for developing bioinspired soft robotics with programmable and reconfigurable functions.

In this review, we provide a state-of-the-art account on recent advances in light-driven bimorphic soft actuators based on photothermal and photochemical effects.[36,37] We firstly aim to introduce the working mechanism of bimorphic soft actuators and promising synthetic strategies towards light-driven soft actuators (Section 2). Photothermal bimorphic soft actuators are then discussed according to optical-to-mechanical energy conversion mechanisms including photothermal-induced expansion, photothermal-induced phase change and photothermal-induced desorption (Section 3). Photochemical bimorphic soft actuators are subsequently discussed with a special emphasis on liquid crystalline and hybrid systems (Section 4). The fundamental design strategies are touched, and their fundamental performance, underlying mechanism and emerging applications are highlighted. In the last section, we conclude a perspective on the exisiting challenges and future opportunities of light-driven bimorphic soft actuators towards their cutting-edge applications. To the best of our knowledge, there are no review which comprehensively introduces such thriving topic of bimorphic soft actuators under one single umbrella, we sincerely feel it is the right time to assemble the scattered literature of this emerging research field which involves a interdisciplinary area including biology, physics, chemistry, engineering, materials science, nanoscience and nanotechnology.

2. Fundamentals of Photoactive Bimorphic Soft Actuators

To endow soft actuators with photoresponsive properties, one can either introduce molecular switches such as azobenzene with light-driven configuration changes or embed functional nanomaterials or dyes with superior photothermal effects into soft matter matrix. Light-driven reversible shape deformation can be only achieved through developing a dynamic stress gradient along the thickness of soft actuators under external light irradiations. Therefore, different approaches have been reported to achieve a desired stress gradient including the soft actuators with homogenous structure,

gradient structure, and bimorph structure (**Figure 1a**). As mentioned above, bimorphic soft actuators that combine an active layer with a passive layer in one single bilayered system could facilitate soft actuators with unprecedented features such as ultrasensitivity, programmability, superior compatibility, robust functionality and easy controllability. It should be noted that bimorphic soft actuators have been powered by various external stimuli such as light,[38,39] temperature,[40,41] humidity,[18] electricity and magnetic field.[24,42,43] In this section, we discuss the bending mechanism of bimorphic soft actuators in general, and then introduce the promising photoactive agents towards light-driven soft actuators.

2.1 Bending mechanism of bimorphic soft actuators

Bimorphic actuators can be traced back to 1925,[44] Timoshenko firstly proposed the systematic theory of bimorph structures, and a uniform curvature can be achieved using two metallic thermostats with different thermal expansion coefficients **(Figure 1b)**. The bending degree of a bimorphic actuator is proportional to the difference in elongation of two layers and inversely proportional to the thickness of the strip, and the bending radius ρ can be expressed by:

$$\rho = \frac{(h_1+h_2)(3(1+m)^2+(1+mn)(m^2+\frac{1}{mn}))}{6(\alpha_2-\alpha_1)(1+m)^2}\frac{1}{(T-T_0)}, \quad m=\frac{h_1}{h_2} \quad , \quad n=\frac{E_1}{E_2}$$

Where T_0 is the room temperature; h_1 and h_2 are the thickness of two layers, E_1 and E_2 denote their moduli of elasticity, α_1 and α_2 represent their coefficients of expansion, respectively.

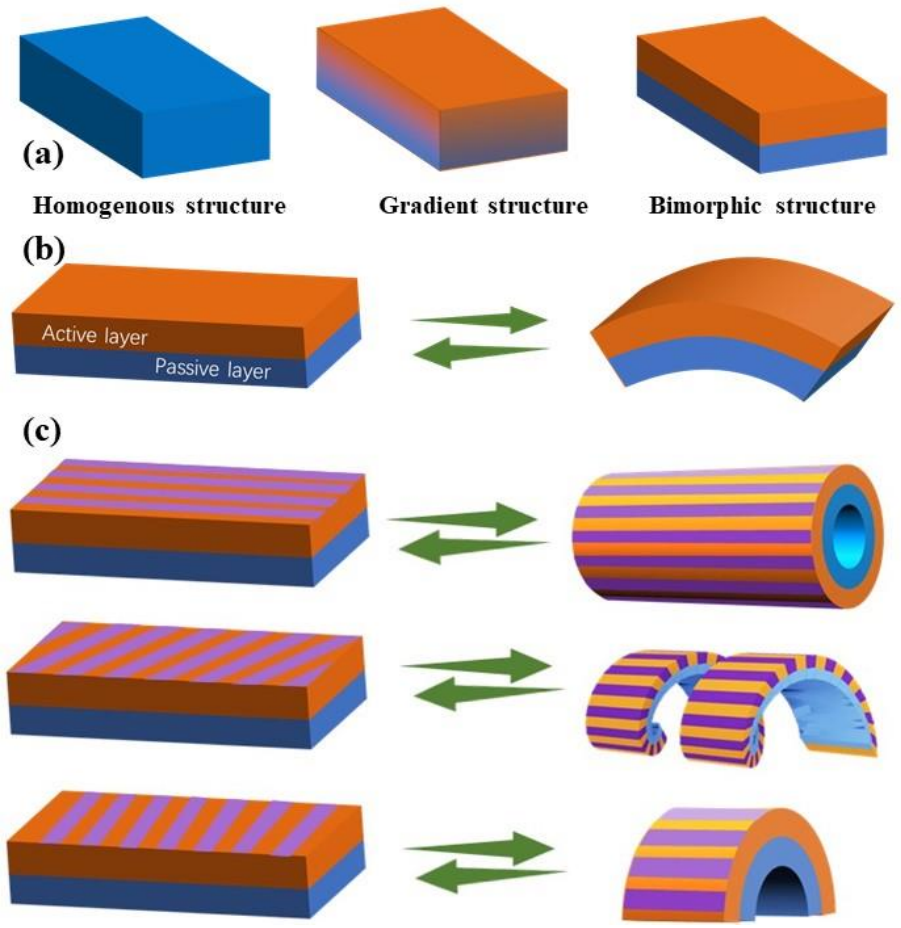

Figure 1. Schematic illustrations showing (a) homogenous structure, gradient structure, and bimorph structure, (b) bending mechanism of bimorphic soft actuators and (c) Programmable spiral twisting deformation of bimorphic soft actuators.

In a photoactive bimorphic soft actuator, the active layer basically dominates the volume change whether it expands or shrinks, and large volume change is often restricted by its mismatch with passive layer, thus resulting in benting deformation in response to external light irradiations. Rational design of bimorphic soft actuator should maximizethe functionalities of both the active and passive layers. It should be noted that multifarious shape deformation such as handness-dependent spiral twisting could be facilely programmed through appropraitely controling the anisotropy direction of two different laminated layers **(Figure 1c)**. However, there is a risk of delamination taking place at the interface between both layers, and a stable and robust interface is a prerequisite for obtaining light-driven bimorphic soft actuators with superior performance. Toward bimorphic soft actuators with a stable interface, several critical

points merit our consideration in the design and fabrication processes. One of the most convenient way is to bond both layers together by the use of pressure sensitive adhesive such as acrylic ester or tape.[45,46] We can also take advantage of some unreacted functional groups on the interfaces to glue both layers together through crosslinking of covalent bonding.[48] Alternatively, we can directly spining-coat the plymeralizable precursors such as PDMS on the surface which could act as a layer after curing.[49,50] Besides, some physical methods could help to strengthen the interfaces between two layers, for example, the plasma treatment could increase the number of polar groups on its surface, which would enable a enhancement in surface wetting ability and bonding between two layers.[51]

2.2 Photoactive agents for bimorphic soft actuators

To obtain light-driven bimorphic soft actuation, one must incorporate photoactive agents such as photothermal nanotransducers (nanoparticles or organic dyes) or molecular photoswitches (azobenzenes) into into soft matter matrix. These photoactive agents can serve to absorb the external light irradiations and facilitate photomechanical actuation through diverse optical processes such as photothermal expansion, photothermal desorption, photothermal phase transition, photochemical configuration changes and beyond. Both photomechanical mechanisms have their own strengths, and could play a distinct role in the development of light-driven bimorphic soft actuators towards advanced light-fuelled soft robots. Herein we aim to provide a brief introduction about different photothermal or photochemical agents and their characteristics.

2.2.1 Photothermal agents

The typical photothermal agents are often devided into two main categories: inorganic and organic photothermal agents. A high photothermal conversion efficiency can be expected in a variety of inorganic photothermal agents including carbon-based nanomaterials,[52] metallic nanoparticles,[53,54] semiconductor nanostructures,[55] transition metal carbide or nitride, etc.[56,57] Carbon-based functional nanomaterials such as

reduced graphene oxide (RGO) and carbon nanotubes (CNTs) have been reported to exhibit high photothermal conversion efficiency and be widely applied as a dispersed agent, an adjacent layer, or a modifier of bimorphic soft actuators.[38,58] Thanks to localized surface plasmon resonance (LSPR), plasmonic nanoparticles such as gold nanoparticles and gold nanorods could selectively absorb the incident light and efficiently convert absorbed light into localized heat.[50] It should be noted that their energy conversion efficiency is closely related to its own size,[59,60] and photoabsorption at a desired wavelength could be facilely achieved through tuning the intrinsic property of plasmonic nanostructures. Recently, MXenes with unique 2D nanostructures have been found to exhibit high thermal conductivity, superior photothermal effect together with hydrophilic feature.[61] For example, Chen *et al.* demonstrated that a photothermal conversion efficiency of 30.3% in MXenes upon NIR irradiation at 808 nm with a intensity of 1 W cm^{-2}.[62,63] Many organic photothermal agents have been widely utilized in the polymeric matrices such as polypyrrole organic polymers,[13] polydopamine,[64] organic NIR absorbing dyes.[65] Compared with inorganic analogues, these organic photothermal agents exhibit much better compatibility with polymeric matrices althrough they show relatively low photothermal conversion efficiency and serious photobleaching.[66] In general, an excellent photothermal agent for bimorphic soft actuators can be evaluated through the following factors: (1) a superior compatibility with soft matter matrix; (2) a broad photoabsorption that could exhibit a tunable absorption spectrum for specific actuation or cover the full solar spectrum range from 250 to 2500 nm toward sunglight actuation; (3) a high photothermal conversion efficiency to ensure an efficient photothermal actuation; (4) synthetic simplicity, good photostability and low cost.[67,68]

2.2.2 Photochemical agents

Photochemical actuation of bimorphic soft actuators is usually achieved by introducing photoswitchable molecules into the active layer based on anisotropic soft matter matrix such as liquid crystal elastomers (LCEs), where light-driven dynamic geometrical

changes of molecular photoswitches or photosensitive chromophores can be autonomously amplified into macroscopic and reversible shape deformation deformation such as bending and curling under the external light irradiations. Many photochromic materials such as spiropyran, diarylethenes and azobenzene derivatives have been reported to show reversible geometrical change under light irradiations at an appropriate wavelength.[69] The spiropyran and spirooxazine can undergo an electrocyclic ring opening reaction from a closed spiro-form to an planar merocyanine form upon UV light exposure. The reversible progress does not happen automatically unless irradiated with visible light or heated in the dark, however, they are very interesting and attractive photochromic materials owing to their excellent photocoloration, strong photofatigue resistance, and fast thermal relaxation.[70] Diarylethenes are known to exhibit a geometrical transformation from a ring-opened form to a ring-closed form under UV irradiations, whereas the reverse process can be only activated by visible light irradiation. Diarylethenes and derivatives have been considered as one of most promising candidates toward optical memory applications thanks to their remarkable thermal stability of both photoisomers, fast photocyclization, and electrical conductivity. Azobenzene and its derivatives are the most widely used photochromic materials in the field of light-driven soft actuators owing to their dramatic difference of molecular configurations at trans and cis states.[71] Irradiated by UV light, azobenzene would convert from the planar trans isomer to the bent cis isomer, and the reversible cis-to-trans isomerization often occurs through the thermal relaxation or irradiation of external light at an appropriate wavelength. These azobenzene derivatives have superior compatibility with polymer matrix and can be facilely integrated into main chain or side chain polymers.[72-74] The light-driven soft actuators based on azobenzene derivatives show fast response and high cycle stability with considerable deformation. In general, robust photoactuation of bimorphic soft actuators can be achieved with a photochemical agent meeting some prerequisites, such as tunable photoabsorption for on-demand actuation, fast response, high sensitivity, fatigue resistance, photostationary states predominantly composed of one isomer.

3. Photothermal Bimorphic Soft Actuators

The mechanism behind the photothermal actuation of bimorphic soft actuators is quite straightforward: the organic dyes or functional nanoparticles loaded into soft matter matrix are able to convert the external light irradiations into *in situ* thermal energy through non-radiative thermal relaxation processes. This localized thermal energy is then transferred into the polymer environment, and results in the light-induced dynamic stress gradient and the subsequent deformation of soft actuators. Herein, light-driven bimorphic soft actuators based on photothermal expansion is firstly discussed, where the photothermal agents could be introduced into the photoactive layer or directly function as a photoactive layer. We then illustrate the bimorphic soft actuators based on photothermal contraction, which could be induced by the photothermal desorption of water or the photothermal phase transition including metal-insulator transition, hydrophilicity-hydrophobicity transition and liquid crystalline nematic-isotropic transition.

3.1 Bimorphic soft actuators based on photothermal expansion

As is well-known, the volume and shapes of most functional materials are closely related to their intrinsic coefficient of thermal expansion (CTE) and would be more or less re-established upon the changes of surrounding temperature. According to the value of CET, we could qualitatively evaluate the degree of volume change of materials upon heating. **Table 1** illustrates the CTE of some representative materials that have been used for soft robotic applications. Bimorphic soft actuators are often fabricated through combing two layers with different CTEs, and the shape deformation can be expected with temperature change. Herein, we introduce some typical bimorphic soft actuators based on photothermal expansion with an emphasis on different photothermal agents, design strategies and fabircation methods.

Table 1. CTEs of representative materials for bimorphic soft actuators.

Materials	CTE [ppm K^{-1}]	Ref.
poly(dimethylsiloxane) (PDMS)	300~310	58

Polyvinylidene Difluoride (PVDF)	127	86
Biaxially Oriented Polypropylene (BOPP)	137	46
Low-Density Polyethylene (LDPE)	>200	47
Polycarbonates (PC)	65	89
Polyethylene Terephthalate (PET)	40	28
Polyimides (PI)	28	34
Poly(methyl methacrylate) (PMMA)	60	91
Paper	10	46
Graphene	-1	75
Single-Wall Carbon Nanotubes (SWCNTs)	-1.5	76
Reduced Graphene Oxide (RGO)	-20	38

3.1.1 Photothermal agents as part of photoactive layer

Light-driven bimorphic soft actuators can be achieved through introducing photothermal agents into the active layer, and this method shows several advantages such as superior photothermal stability and high photothermal conversion efficiency. It should be noted that photothermal agents homogeneously dispersed in soft matter matrix can not only play a critical role in efficient photothermal conversion, but also contribute to the changes in the CTE and Young's modulus of active layer. For example, Jiang *et al.* incorporated 5 wt% graphene nanoplatelets (GNPs) with PDMS to construct PDMS-GNPs/PDMS bimorphic soft actuators,[77] where the introduction of GNPs made the difference of CTE and Young's modulus between pure PDMS passive layer and PDMS/GNPs active layer. Wang *et al.* found that the degree of shape deformation and response speed of PDMS-GNPs/PDMS bimorphic soft actuators could be controlled by varying the doping concentration of graphene nanomaterials.[47] Tang *et al*. developed the bimorphic soft actuators that consisted of a passive layer of pure PDMS and an active layer of PDMS composites with reduced graphene oxides (RGO) and thermally expanding microspheres (TEMs).[55] It was found that that the introduction of TEM

significantly enhanced the CTE of PDMS. Upon NIR light irradiations, the effcient photothermal RGO enabled a rapid temperature increase from 20 ℃ to 110 ℃ in 30 s, and a subsequent large volume increase of TEM yielding 350% diameter and 4000% volume changes in 15 s. As a result, the bimorphic soft actuators ($20 \times 2 \times 1.4$ mm^3) were able to bent toward the PDMS side into almost semicircular (180°), which were further used as active hinges to develop light-driven self-folding 3D architectures with arbitrary shape (such as cars, boxes and pyramids). Leeladhar *et al.* developed light-fueled reversible GNP-PDMS/Au tubular bimorphic soft actuators with large shape deformation and fast response speed by doping GNPs into PDMS matrix,[78] and the resulting three-dimensional tubular soft actuators was able to transform into a two-dimensional sheet within 8 s under NIR light irradiations. Interestingly, Lim *et al.* developed a light-driven venus flytrap based on polypropylene (PP) /PDMS bimorphic soft actuators,[79] where active layer of PP was doped with poly(3,4-ethylenedioxythiophene) (PEDOT) exhibiting superior photothermal properties, the large CTE mismatch of PP and PDMS ensured an ultrasensitivity and significant shape-shifting upon external light exposure, and the photothermally driven reversible shape-folding with large deflection up to 150° and displacement of >20 mm were achieved by appropriately controlling the thickness of each layer. Such PP-PEDOT/PDMS bimorphic soft actuators with large actuation are expected to generate complex chaotic architectures with programmable capability that could find promising applications in areas of biomedical devices, microfluidic devices, aerospace and beyond.

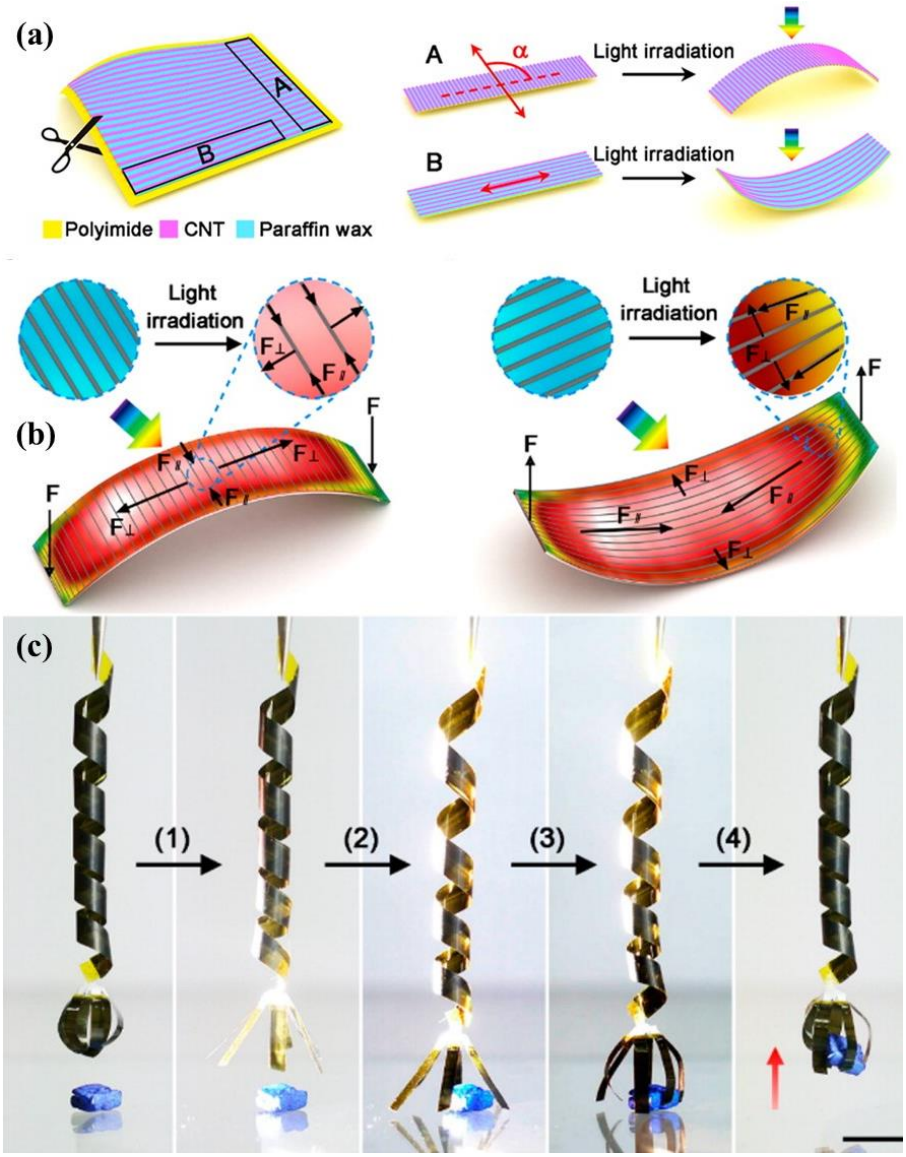

Figure 2. Light-driven bimorphic soft actuators with programmable deformations by embedding aligned CNTs in paraffin wax on a polyimide substrate. a) Apheliotropic and phototropic bending of bimorphic soft actuators with different aligned directions of CNTs. b) Schematic mechanism of apheliotropic bending and phototropic bending. c) Photographs of light-driven mechanical arm based on bimorphic soft actuators. Reproduced with permission from ref. 34. Copyright© 2016, 2014, American Chemical Society.

In general, light-driven uniform expansion or contraction are often observed in bimorphic soft actuators with photothermal nanomaterials randomly dispersed in the active layer. Controled alignment of anisotropic nanoagents such as aligned carbon nanotubes (CNTs) is much prefered to achieve more complex and programmable deformation of soft actuators.[80] Inspired by opening movement in pine cones and 3D twisting motion in *Bauhinia variegata* pods, Deng *et al.* demonstrated light-driven

bimorphic soft actuators with programmable deformations by embedding aligned CNTs in paraffin wax on a polyimide substrate, where the aligned CNTs that function as cellulose fibrils are used as geometrically constraining structures on the expansion of paraffin wax mimicking the soft tissues of a plant **(Figure 2a, b)**.[34] Interestingly, such soft actuators cutting along different CNT orientations could exhibit complex, reversible and repaid deformation upon the visible light. The angle α is defined as the difference between the longitudinal direction of the strip and the CNT orientation. When α = 90°, an apheliotropic bending angle of ~85° was observed upon light irradiation, while a phototropic bending angle of ~60° when α = 0°; In contrast, light-driven reversible right- and left-handed helical transformations were respectively observed when α = 45° and 135°. They further developed a mechanical arm with real-time and remote controllability through combining bending and helical deformations of bimorphic soft actuators, where the claw opened and the telescopic arm elongated upon light irradiations. When the light was removed, the claw grasped and catched an object, and the telescopic arm contracted and lifted the object up **(Figure 2c)**. It is worth noting that light-driven dynamic actuations can be accomplished in milliseconds and soft actuators exhibited excellent fatigue resistance after 100 000 working cycles.

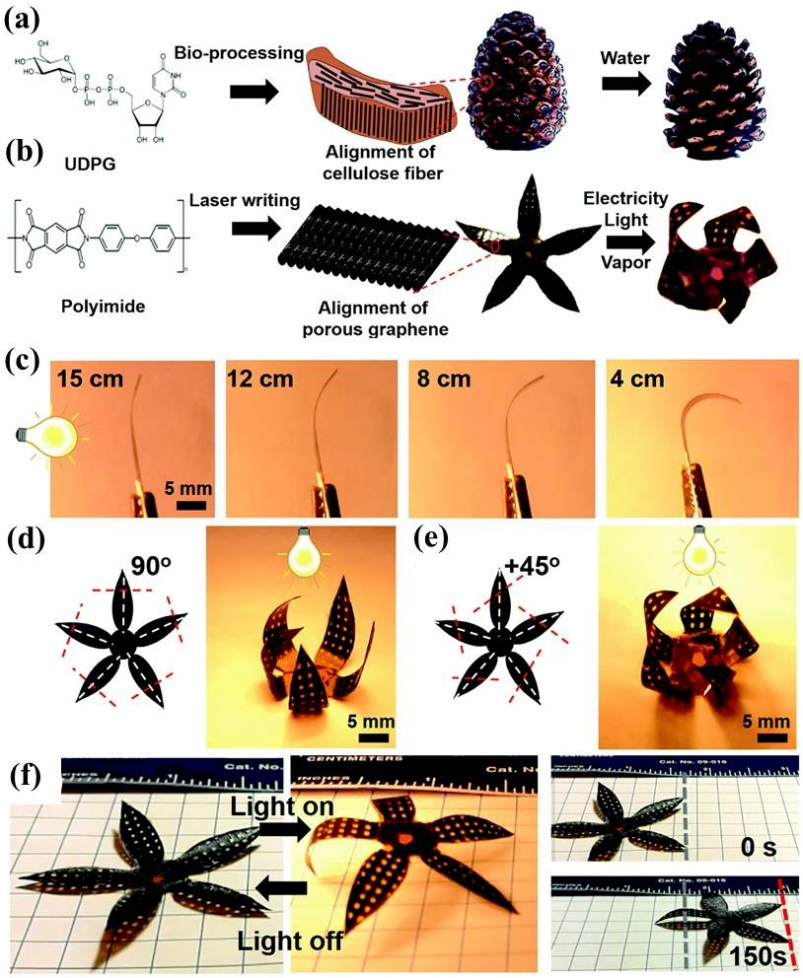

Figure 3. Bioinspired light-driven PVDF/LIG/PI soft actuators controlled by laser tailored graphene structures. a) Mechanism of reversible opening and closing state of a pine cone. b) Schematic alignment of LIG using the DLW method and light-driven dynamic function of soft actuators. c) Photographs of PVDF/LIG/PI soft actuators under light exposurewith different distances. d), e) Photographs of a flower-shaped soft actuator with different LIG alignment angles. f) A light-driven five-legged crawling soft robot.[81] Reproduced with permission from ref. 81. Copyright© 2018, Royal Society of Chemistry.

Plants are known to exhibit stimuli-driven complex shape deformation with the aligned cellulose fibrils as geometrically constraining elements **(Figure 3a)**, Deng *et al* fabricated aligned laser induced graphene (LIG) patterns by a one-step direct laser writing (DLW) method, and demonstrated light-driven PVDF/LIG/PI soft actuator through sandwiching LIG between an active PVDF polymer and a passive PI polymer **(Figure 3b)**.[81] The active PVDF layer exhibited strong solvent swelling ability and large coefficient of thermal expansion. The aligned LIG can not only serve as a geometrically constraining structure to inhibit the expansion of the PVDF in the

alignment direction, but also function as a effcient photothermal agents that stimulate expansion of the PVDF upon light irradiations. The bending curvature of resulting soft actuators could be varied through changing its distance with the lamp **(Figure 3c)**, and different shape deformation geometries of soft actuators could be achieved based on the geometrically constraining effect from the aligned LIG structures. For instance, upon changing the LIG alignment angle from 90° to 45°, the flower-shaped soft actuator was found to show different reversible shapes from bending to helical curling under external light irradiation **(Figure 3d, e)**. Interestingly, the authors demonstrated a miniature light-driven five-legged soft robot made from LIG with an alignment angle of 90°, which can move away from the light source since the five legs receive different photon energy according to their distances from the lateral lamp **(Figure 3f).** The strategies disclosed herein could provide new insights into the development of bioinspired soft actuators or machines with complex and reconfigurable motion towards novel multi-functional electronic and photonic devices for a wide variety of promising applications, such as soft robotics, artificial muscles, sensing and beyond

3.1.2 Photothermal agents directly as photoactive layer

Many photothermal polymers and nanomaterials are found to exhibit both outstanding photothermal conversion efficiency and low or even negative CTEs, such as CNTs,[82] graphene,[83] polypyrrole,[84] nanocrystalline metal.[85] Therefore, these advanced photothermal nanoagents have been directly used as a passive layer of light-driven bimorphic soft actuators.[86-88] For example, Tai *et al.* developed light-driven rapid-response single-walled carbon nanotube (SWCNT)-polyvinylidene fluoride (PVDF) bimorphic soft actuators, where the fast, powerful photodriven actuation performances are believed to result from the negative CTE and high coefficient-of-hygroscopic-expansion (CHE) of SWCNT layer as well as high CTE and low CHE of the PVDF layer.[86] Yang *et al.* demonstrated an autonomous CNT/PDMS bimorphic soft actuator with a curled droplet shape, and continuous wavelike self-oscillation was observed upon continuous external light irradiation.[87] Such unique cyclic wavelike oscillating

motion was enabled through a light-to-mechanical negative feedback loop including light-fueled actuation, photothermal response delay along the direction away from light source and superior mechanical elasticity of soft actuators. It should be noted that the cyclic oscillating motion with different frequency and amplitude could be faciely achieved by changing the exposure intensity and incident direction of external light. Interestingly, a self-locomotive artificial snake with phototaxis was also demonstrated, which could continuously crawl toward the light source with constant irradiation. Thanks to the unique self-sustained rocking motion with constant light irradiation, these bimorphic soft actuators could find a variety of promising applications in areas of advanced bioinspired soft robots, optical-energy-harvesting devices and beyond.

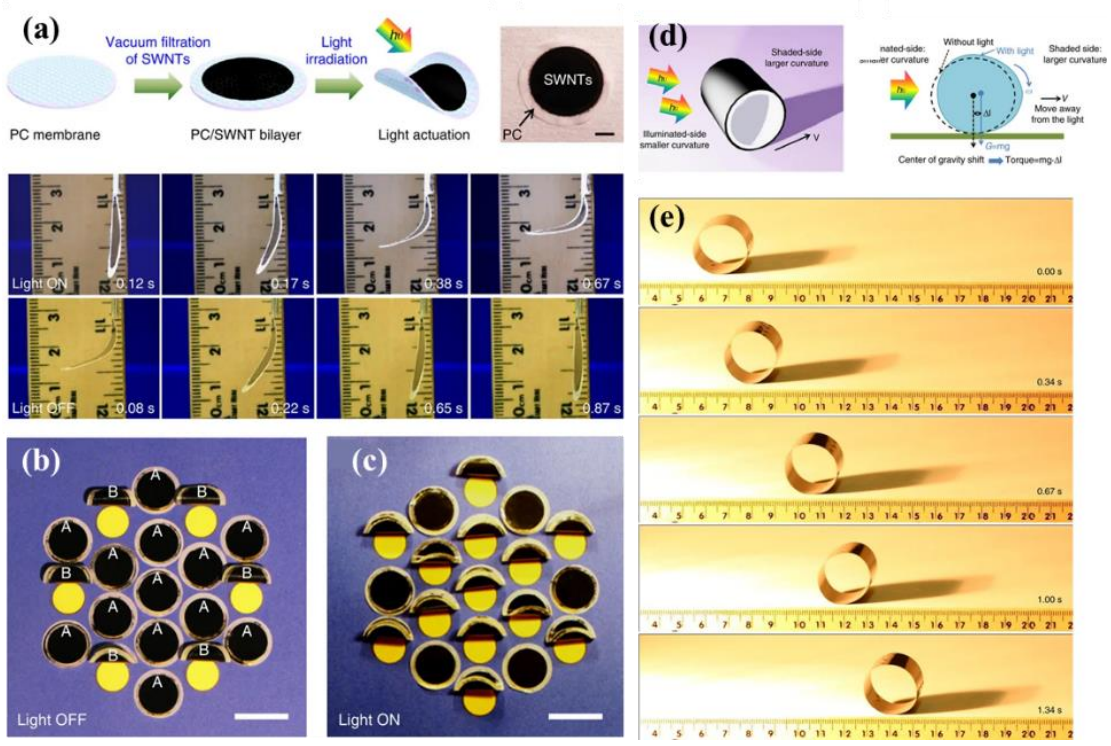

Figure 4. Light-driven SWNT/PC bimorphic soft actuators. a) Schematics of fabricating PC/SWNT bilayer structure and light-driven actuation. b, c) Smart curtains based on bimorphic soft actuators. d) Schematic working mechanism of PC/SWNT bimorphic macro-scale motors. e) Optical image of light-driven forward-moving motor. Reproduced with permission from ref. 89. Copyright© 2014, Nature Publishing Group.

Inspired by instantaneously releasing large elastic energy and force output upon flicking human's finger, Hu *et al.* developed, a soft jumping robot based on CNTs/PDMS bimorphic soft actuators mimicking the gymnast's somersault, where

CNTs were used as photothermal agents and passive layer simultaneously.[90] The remarkable performances of resulting light-driven soft actuators such as fast response (< 5 s) and ultralarge deformation (angel change >200° and curvature > 2 cm^{-1}) were found to result from the large mismatch of CTEs between CNTs and PDMS, high optical absorption of CNTs, loosely network of CNTs, as well as stable and durable CNT-polymer interface. Zhang *et al.* reported a robust light-driven SWNT/polycarbonate (PC) bimorphic soft actuators with large deflection, fast response speed and extreme light sensitivity.[89] The bimorph structures were fabricated through vacuum filtration of a SWNT solution on a 10-mm-thick PC membrane with a 0.4 mm pore size **(Figure 4a)**. It was found that the responsive wavelength range of resulting bimorphic soft actuators could be readily programmed by changing chirality distribution of SWNTs since the light absorption characteristics of CNTs are closely related to their chiralities. Upon constant light irradiations, the PC/SWNT bimorphic soft actuators were also found to oscillate around its saturation bending angle with a frequency of ~5Hz due to the shadowing effect. Interestingly, the concept of 'smart' curtains was demonstrated using this unique bimorphic soft actuators, which could open or close under sunlight exposure **(Figure 4b, c)**. The author also developed PC/SWNT bimorphic macro-scale motors with fast mechanical motion driven by external light irradiations. Non-uniform illumination on the motor from an angled light source resulted in the decreasing curvature on the light-facing side. As a result, the location that gets more illumination tends to be flattened, which resulting in a change to the centre of mass of the motor, and a subsequent torque that drives the motor away from light on a flat surface at a speed of ~6 cm s^{-1} **(Figure 4d, e)**. These results are expected to open new door for the development of complex and reconfigurable structures using a scalable process towards the emerging application in areas of soft robots, biomimetic devices and many other systems in satellite and spacecraft.

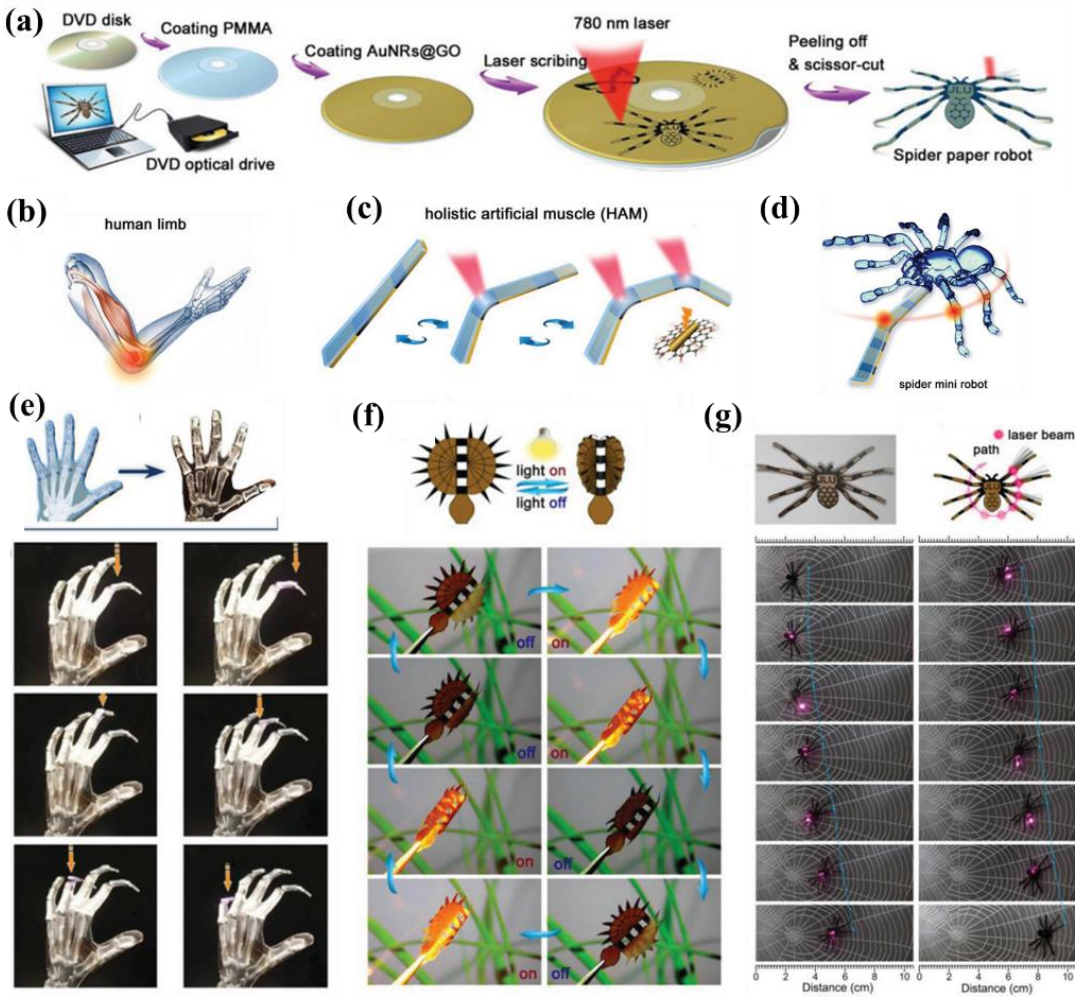

Figure 5. Laser-printed holistic artificial muscle based on PMMA and AuNRs@GO nanocomposite bimorphs. a) Schematic illustration of fabrication process. b) A human arm whose actions are realized through a combined work of skeletons and muscles. c, e) Light-driven artificial muscle and light-driven artifical hand. f) Light-driven artifical Venus flytrap. g) Light-driven artifical spider. Reproduced with permission from ref. 91. Copyright© 2019, Wiley-VCH.

Many researchers are devoted to developing light-driven bimorphic soft actuators with enhanced performance and functionality by combining different photothermal agents into one single layer. Hu *et al.* reported RGO-CNT/PDMS bimorphic soft actuators with RGO and CNTs as passive layer.[92] It was found that the pure RGO-CNT monolayer could qucikly reach a maximum temperature of 100 °Cupon external light irradiation (250 mW cm^{-2}), resulting in an angle change of soft actuator from 84° to 563° in 3.6 s. Interestingly, a light-fueled crawler-type robot was fabricated with RGO/-CNT/PDMS bimorphic soft actuators, which could perform fast and sophisticated

function mimicing the tank track motion under external sunlight exposure. Besides carbon-based nanomaterials, some plasmonic nanoparticles such as gold nanorods (AuNR) exhibit high photothermal efficiency, and their longitudinal surface plasmon resonance (LSPR) could be faciely controlled across a broad spectral range.[93] Han *et al*. reported a laser-printed holistic artificial muscle (HAM) made from a AuNRs@GO nanocomposite layer and a thermally expansive PMMA polymer layer.[91] To fabricate this light-driven artificial muscle, PMMA and AuNRs@GO nanocomposite were firstly coated onto a light-Scribe-enabled DVD in sequence, and laser scribing was utilized to write thermal conductive nodes on the AuNRs@GO layer in the light of computer-designed patterns. The light-driven bimorphic soft actuators with different functionalities was then peeled off the DVD followed by boundary cutting, which can be used as holistic artificial muscle (**Figure 5a-d**). For example, a set of hand skeletons was fabricated by integrating a prepatterned HAM into PDMS (**Figure 5e**), and light-driven dynamic hand manipulation was achieved since every node of hand could be freely controlled in a noncontact manner. Interestingly, light-driven Venus flytrap and spider soft robotics were also demonstrated. The artifical Venus flytrap could capture and release an object through switching a laser beam on and off (**Figure 5f**). The 2D-patterned artifical spider could deform into 3D structures with legs seperately controlled upon external light irradiation, thus they could walk freely through remote manipulation using one or more laser beams (**Figure 5g**). The nanofabrication strategy presented herein is expected to bridge the gap between ideal requirement and realistic limitations of bioinspired soft actuators, which could find important applications in diverse fields from soft robotics to human-machine inteface technologies.

3.2 Bimorphic soft actuators based on photothermal contraction

The CTE value of functional materials can be positive or negative. Thermal expansion is often observed in materials with positive CTE, while thermal contraction or shrinkage occurs in materials with negative CTE. It has been reported that many advanced functional materials could undergo a contraction across the entire volume or in a certain

direction of the volume, such as graphene,[83] poly(N-isopropylacrylamide) (PNIPAM),[94,95] and aligned liquid crystalline elastomer.[96] Extensive efforts have been recently made to develop light-driven bimorphic soft actuators based on photothermal contraction, and the mechanism of photothermal contraction mainly includes photothermal desorption and photothermally indeced different phase transitions such as metal-insulator transition, hydrophilicity-hydrophobicity transition and nematic-isotropic transition. In this section, we introduce recent advances in bimorphic soft actuators based on photothermal contraction.

3.2.1 Contraction induced by photothermal desorption

Many advanced nanomaterials and functional polymers are know to have a plenty of hydrophilic groups that can adsorb water molecules significantly when exposed to moisture. Upon increasing tempertature or photothermal irradiations, these materials often exhibit a volume contraction or shrinkage because of the reversible adsorption and desorption of water under the environment with high humidity. For example, graphene oxide (GO) with abundant oxygen-containing groups were found to be highly sensitive to environmental humidity since they provide many hydrophilic sites for reversibly ultrafast water adsorption/desorption.[97,98] When the temperature is increased, the desorption of water will take place between adjacent GO sheets, resulting in the vertical collapse and transverse contraction.[98-101] Yang *et al.* developed GO-polydopamine (PDA)-gold nanoparticles (AuNPs)/PDMS bimorphic soft actuators that integrate photothermal expansion of PDMS layer and photothermal water loss or shrinkage of GO-PDA-AuNPs layer.[51] It was found that theactuating efficiency of such soft actuator could be dramatically enhanced compared with that of conventional one. Zhang *et al.* designed and fabricated bimorphic soft actuators that exhibited bi-directional bending actuations upon exposure to light irradiation or humidity (**Figure 6**).[100] The bimorphic structure consisted of a GO layer and a composite layer of nano-size graphite (Nano-G) and polyvinylidene fluoride (PVDF) as show in **Figure 6a**. GO is an active layer responsive to moisture and Nano-G@PVDF is a passive layer (**Figure**

6b). In addition, Nano-G@PVDF layer with a relatively large CTE is active under light irradiation, and GO layer is passive due to its low CTE. Taking advantage of complemental moisture and photothermal actuations, the authors developed a bi-directional walking robot that can move along the Y direction upon external light irradiations and move along the X direction in response to the humidity (**Figure 6c**). A square-shaped paper was used as main body of such walking robot with eight Nano-G@PVDF/GO bimorphic soft actuators as legs. Four pairs of legs were divided into two group, that is, one with GO as upper layer and the other with Nano-G@PVDF as upper layer. When the robot was exposed to the moisture of ~ 100%), the walking legs were found to bend toward the Nano-G@PVDF side. As a result, the legs with Nano-G@PVDF as upper layer bend upwards, and the legs with GO as upper layer bend downwards. Upon changing the environmental humidity, the walking robot move toward the X axis direction with the legs bent downside and recover alternately (**Figure 6d**). Interestingly, under the environment with constant humidity, external light irradiation can driven the upwards bending of legs one with GO as upper layer and the downwards bending of legs with Nano-G@PVDF as upper layer. The walking robot could move along the Y axis direction through appropriately switching on and off the light irradiations (**Figure 6e**). Moreover, Dong *et al.* developed programmable GO-polypyrrole (PPy) bimorphic soft actuators that exhibited superior actuating performance in response to humidity, temperature, and light irradiations owing to the different water adsorption or desorption capability between GO and PPy.[99-101] Inspired by tendril climber plants, light-driven smart grippers with helical structures were demonstrated to capture and release target objects. A soft walking robot based on GO-PPy bimorphic soft actuators can mimickg the movement of the inchworm moving forward for a long distance under the interval light irradiations. These unprecedented strategies could provide a robust and versatile method for developing advanced and programmable soft robotics with truly bioinspired intelligence.

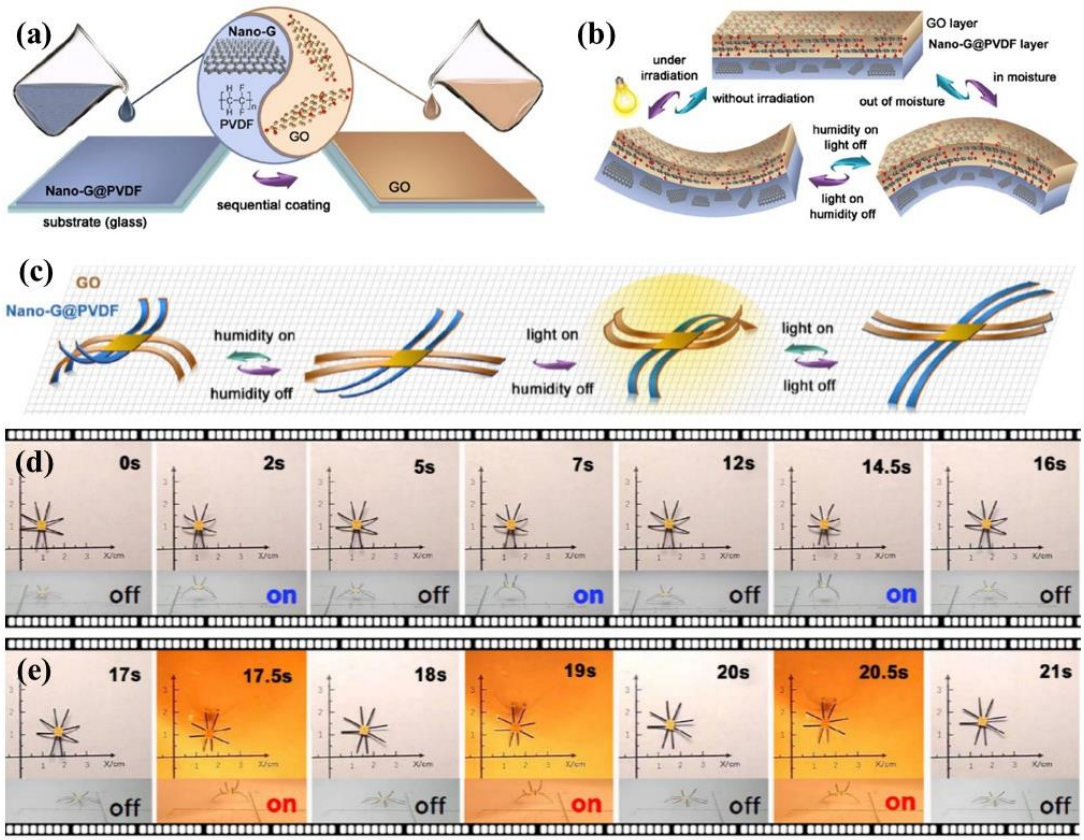

Figure 6. Bimorphic soft actuators with exhibit bi-directional bending actuations. a) Schematic fabrication process of Nano-G@PVDF/GO bilayer film. b) Schematic actuation mechanism of Nano-G@PVDF/GO soft actuators. c) Bi-directional walking robot that can move along different directions in response to environmental humidity and external light irradiation, respectively. d) Soft robot walking toward the X axis direction upon changing the environmental humidity. e) Soft robot walking along the Y axis direction upon switching on and off the light irradiations. Reproduced with permission from ref. 100. Copyright© 2020, Elsevier.

Gao *et al.* demonstrated the design and fabrication of photothermal actuated complex origamis based on GO-ethylene cellulose (EC) bimorphic soft actuators,[102] which was fabricated by patterning GO onto EC substrate in a heterogeneous manner (**Figure 7a**). The CTE value of GO is highly related to reversible removal/intercalation of water between adjacent atomic layers, and negative CET is often obersved in a humid environment. When combined with EC exhibiting highly positive CTE, the large CTE mismatch endowed GO-EC soft actuators with intensive deformation and fast actuation. It should be noted that GO can not only act as a photothermal agent, but also enable programmable shape deformation of soft actuators through appropriate alignment. The authors demonstrated many different shape programmable 3D architectures based on

GO-EC bimorphic soft actuators such as triangular rings encoded with positive or negative curvatures and annulus rings with central or axial symmetry as well as mechanical metamaterials encoded with positive or negative Poisson's ratio (**Figure 7b-e**). Importantly, these complex 3D origamis can be reversibly actuated toward transformation between their 3D models and flattened 2D states upon external light irradiations. Interestingly, light-driven dynamic bloom of bioinspired origami flower was also demonstrated, where the artificial flower could mimic a series of intermediate blossom and fully flattened states through applying NIR light with different intensity (**Figure 7f, 7g**). Moreover, Humidity- and light-driven bimorphic soft actuators that combined different carbon nanomaterials such GO-CNT and GO-RGO were reported to enable unprecedented actuating performaces such as ultrafast response, high reversibility ultralarge deformation as well as on-demand control over deformation direction.[103-107] These strategies are expected to offer new insights into the development of light-driven bimorphic soft actuators with tunable functionalities for various promising applications such as soft robotics, mechanical metamaterials, and other bioinspired artificial and intelligent nanosystems.

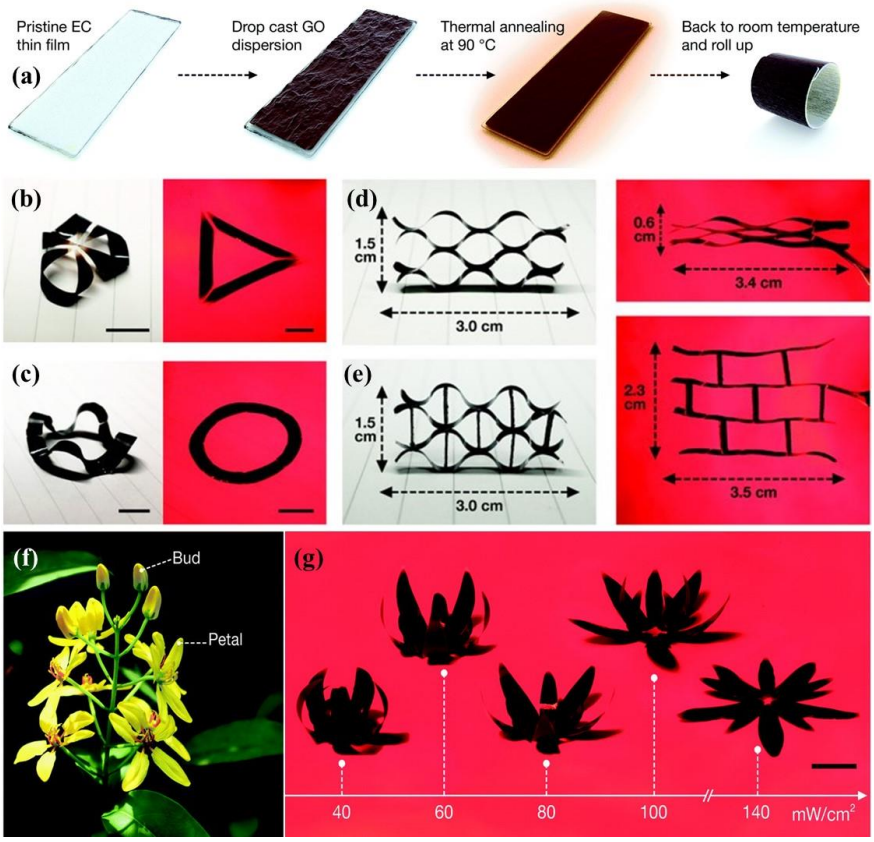

Figure 7. Light-driven complex origamis based on GO-EC bimorphic soft actuators. a) Schematic illustration of fabrication process. b) Triangular ring encoded with positive negative curvature. c) Annulus ring encoded with central symmetry. d, e) Mechanical metamaterials encoded with positive and negative Poisson's ratio, repectively. f) Natural buds and flowers of gold climber (Tristellateia australasiae A. Rich). g) Light-driven dynamic bloom of bioinspired artificial origami flower. Reproduced with permission from ref. 102. Copyright© 2020, Royal Society of Chemistry.

Taking advantage of extraordinary water adsorption/desorption capacity of cellulose-based functional materials, Weng *et al.* fabricated humidity- and light-driven graphite-paper bimorphic soft actuators through deposition of graphite so called pencil-on-paper approach.[46] Cai *et al.* reported an leaf-inspired asymmetric bimorphic soft actuators with 2D Mxene-cellulose composites coated onto polycarbonate (PC) membrane (**Figure 8**), which could mimic not only the sophisticated nanoarchitecture of natural leaf toward swelling and shrinking upon water sorption and desorption, but also exhibit solar-harvesting and energy-conversion functionalities.[63] MXene and cellulose nanocomposite ink was prepared and then filtered onto porous PC membrane for fabricating asymmetric soft actuators, where biocompatible cellulose nanofibers

were used to enable robust and rapid shape deformation and PC membrane could facilitate water insertion/extraction into/from the MXene-cellulose nanocomposites. It was found that MXene and nanocellulose can readily be associated and dissociated with small humidity fluctuations thanks to the abundant existing of hydrophilic functional groups on their surface. Due to excellent photothermal properties of 2D Mxene, the resultant bimorphic soft actuators were found to exhibit autonomous and reversible shape-bending deformation upon changing the environmental humidity and external light irradiations (**Figure 8a-d**). The authors also demonstrated programmable soft actuators with 2D Mxene-cellulose coating as active hinges, and a variety of sophisticated light-driven actuating structures were developed by designing different hinges on PC membrane such as U-shape curvature, "trefoil arch" shape andself-folding box (**Figure 8e-g**). For example, the active hinges of self-folding box could autonomously fold themselves upon NIR light irradiations, the resulting box would unfold back into its original state after tuning of light exposure. These bioinspired adaptive soft actuators when integrated with advanced sensing systems[104] are expected find promising applications in areas of soft robotics, information encryption, smart camouflage, human-machine interface and many emerging intelligent wearable technologies.

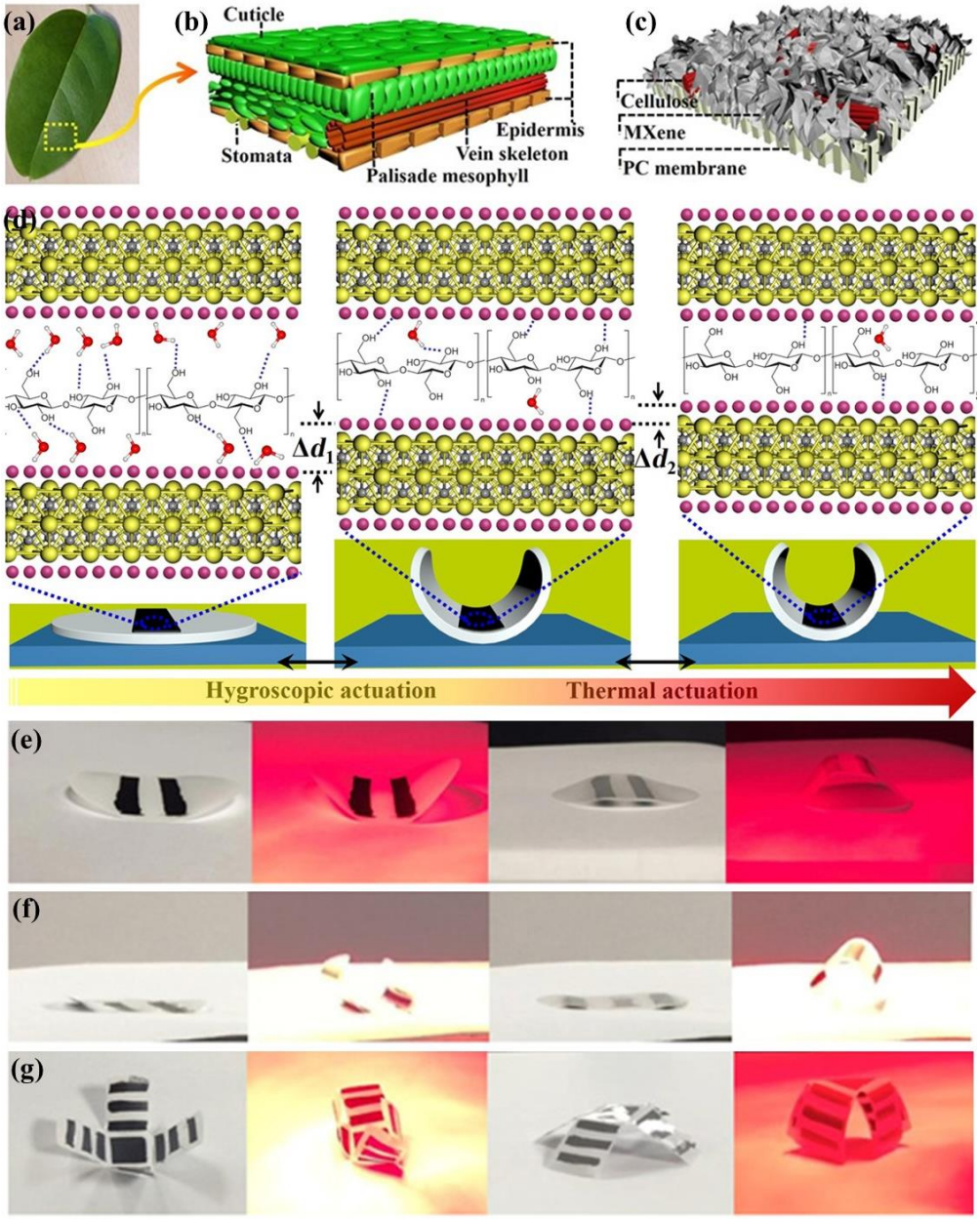

Figure 8. Leaf-inspired MXene/cellulose-PC bimorphic soft actuators. a, b) A natural leaf and its sophisticated nanoarchitecture. a,d) Schematic structure and actuating mechanism of Mxene/cellulose-PC bimorphic soft actuators. Light-driven shape-programmable bimorphic soft actuators: e) U-shaped curvature, f) "trefoil arch" shaped actuator, and g) self-folding box.[63] Reproduced with permission from ref. 63. Copyright© 2020, American Association for the Advancement of Science.

Besides cellulose-based functional nanomaterials, many materials systems with abundant oxygen-containing groups have been used for fabrication of light-driven soft actuators. Li *et al.* developed light-driven bimorphic soft actuators consisted of carbon black photothermal agents, waterborne acrylic adhesive swelling/shrinking layer and

and polyethylene terephthalate (PET) film passive layer.[28] Ji *et al.* reported light-driven robust bimorphic soft actuators based on polydopamine-modified reduced graphene oxide (PDA-RGO), which was prepared by spin-coating UV-cured Norland Optical Adhesive (NOA)-63 onto PDA-RGO layer.[64] Upon NIR light irradiations, the hydrophilic PDA-RGO layer was able to swell/shrink by absorption/desorption of water, resulting in efficient bending/unbending motions of the PDA-RGO/NOA-63 bimorphic soft actuators thanks to the rational combination of the strong adhesion, superior hydrophilicity, thermal conductivity and photothermal conversion of PDA and RGO sheets. Tu *et al.* demonstrated TiO_2-patterned Agarose@CNTs/Agarose bimorphic soft actuators, where CNTs acted as photothermal agents and the hydrophilic groups of Agarose enabled extraordinary swelling/shrinking capacity.[105] TiO_2 pattern with high refractive index could not only help shape-programming such as left-hand and right-hand twisting, but also partly reflect light irradiations toward spatially-selective photothermal actuations. Zhang *et al.* utilized $CaCl_2$ aqueous solution to pattern the surface of sodium alginate/PVDF bimorphic soft actuators, thus obtaining humidity- and sunlight-driven programmable shape-deformations.[101] Undoubtedly, these strategies taking advantages of unique functional materials have greatly promoted the performance of light-driven bimorphic soft actuators with versatile and complex motions, more innovative measures could be taken into account to be implemented for different application fields such as improving the mechanical strength with inorganic materials, such as metals, semiconductors and other novel nanocomposites.

3.2.2 Contraction induced by photothermal phase transition

Many functional materials are known to exhibit various phase transion (such as metal-insulator transition, hydrophilicity-hydrophobicity transition and nematic-isotropic transition) at a certain temperature, which could lead to discontinuous volume change of materials and subsequent contraction of resulting bimorphic soft actuators. Metal-insulator transition (MIT) can be often observed in a well-known thermochromic material vanadium dioxide (VO_2). For example, the lattice structure of VO_2 would

transform from the monoclinic (insulating, I) to the rutile (metallic, M) when the temperature is above 68 °C (**Figure 9a**), such unique transition could result in contraction of ε ~ 1% along the c-axis of the rutile phase.[107-109] It should be noted that the volumetric work density of VO_2 is up to 7-28 J/cm^3 with a high elastic modulus of ~140 GPa, which is 3 orders of magnitude higher than human muscles (~ 0.008 J/cm^3).[109] Importantly, VO_2 was found to exhibit superior energy efficiency (7.7%) and intrinsically fast transition process.[110,111] Liu *et al.* reported Cr/VO_2 bimorphic soft microactuators with photolithography technique,[104] which exhibited a large change in curvature upon the MIT of VO_2 at the temperature of 68 °C. Many efforts have been made to reduce the MIT temperature and improve the efficiency of VO_2-based soft actuators by VO_2 doping or deposition prestressed VO_2 film on some specific substrates.[112-114] Wang *et al.* integrated the high photothermal absorption of SWNTs on the surface of VO_2 (**Figure 9b**),[115] it was found that SWNT/VO_2-based soft actuator could be effciently powered with approximately half the power of bare VO_2-based soft actuators (6.0×10^4 mW/cm^2). Ma *et al.* lowered the MIT temperature of VO_2 at approximately 34 °C through doping 1.5 at % W into the VO_2 film.[116] Upon integrating with SWNTs, the actuation power of this W-VO_2/SWNTs soft actuator was significantly decreased to 250-800 mW/cm^2 with a response time of ~28.5 ms. Recently, Chen *et al.* developed anisotropic super-aligned VO_2 nanowire array (NA)/CNT bimorphic soft actuators (**Figure 9c,d**).[117] Interestingly, a large strain of ~0.614% close to that of single-crystalline ones was achieved along the longitudinal direction, and the resulting VO_2 NA/CNT bimorphic soft actuators many other superior actuation performances such as fast response of ~15 Hz, a giant displacement/length ratio of 0.83, high work density of 2.64 J cm^{-3}, and long lifetime of more than 1 000 000 actuation cycles. Taking advantage of cutting direction-dependent bending morphologies with VO_2 NA/CNT bimorphic structures, light-powered insect-scale soft robots have been demonstrated to exhibit multiple functions such as biomimetic lifter and gripper, soft crawlers as well as wings of flying robots (**Figure 9e,f**). These

strategies could pave the way for the development of versatile light-driven insect-scale soft robotics with extensive mechanical applications.

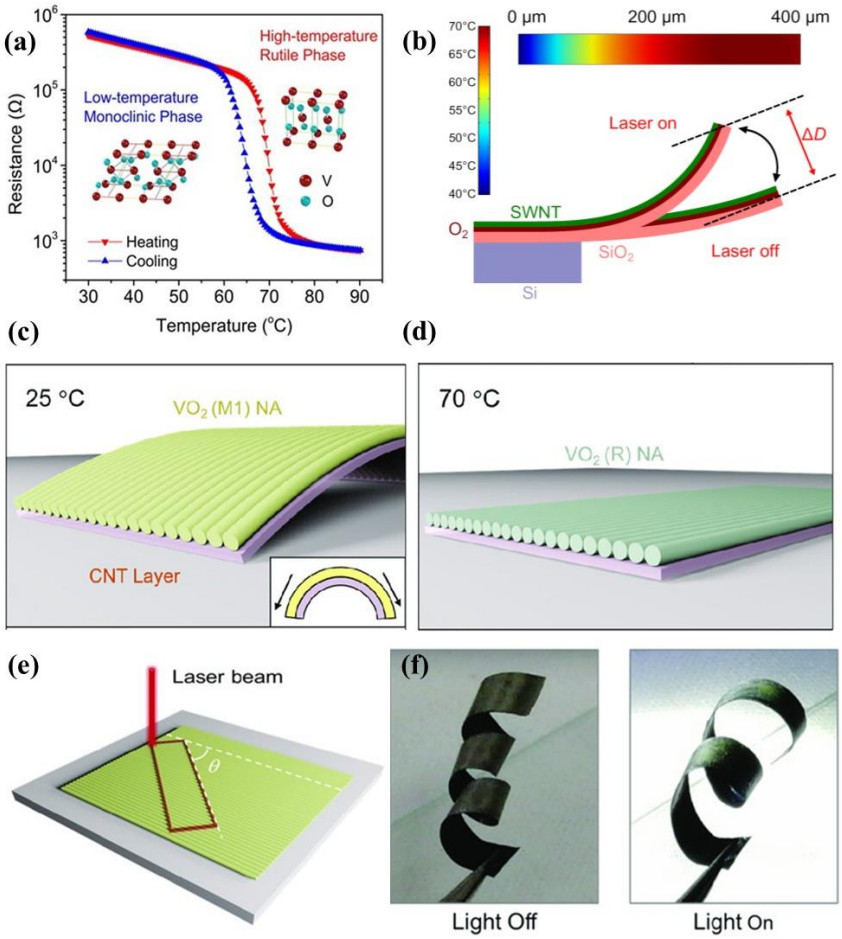

Figure 9. VO_2-based bimorphic soft actuators. a) Resistance change of VO_2 as a function of temperature. b) Schematic of SWNT/VO_2-based soft microactuator and COMSOL simulation. Reproduced with permission from ref. 115. Copyright© 2015, American Chemical Society. VO_2 NA/CNT bimorphic soft actuators at different temperature: c) 25 °C, d) 70 °C. e) Schematic of fabricating VO_2 NA/CNT bimorphic soft actuators by a laser beam with an adjusted cutting angle (θ). f) Helical twisting of VO_2 NA/CNT bimorphic soft actuators with θ=45° under strong light illumination. Reproduced with permission from ref. 117. Copyright© 2020, Wiley-VCH.

Poly(N-isopropylacrylamide) (PNIPAm) is known to exhibit hydrophilicity-hydrophobicity transition, where the polymer segments of PNIPAm could be hydrated, swollen or open below a lower critical solution temperature (LCST) of ~32°C, whereas they would convert to become more compact, shrunken or collapsed above the LCST.[118] It shoud be noted that PNIPAm could shrink with a volume variation of ≈90% from a hydrophilic state to a hydrophobic state,[119] which have been promising candidates for light-driven bimorphic soft actuators. Kim *et al.* reported light-driven

bimorphic hydrogel actuator using PNIPAm/rGO as the active layer and polyacrylamide (PAAm) as the passive layer.[120] Thanks to the superior high compatibility and water dispersibility of GO with hydrogels,[121] the authors were able to chemically reduced the GO sheets *in situ* in the hydrogel network, thus avoiding aggregation problem of rGO in hydrogels. As shown in **Figure 10a**, there is a complete difference in the linear swelling ratio between PAAm and PNIPAm-rGO composite. The as-prepared PNIPAm/rGO could undergo a volume contraction upon external light irradiations owing to the enhanced photothermal efficiency of rGO. Interestingly, a light-driven bidirectional motion of turning inside out could be achieved throught tuning the swelling ratio of each layer in the initial state (**Figure 10b**), and the actuation behavior can be manipulated independently by local light irradiation (**Figure 10c**). Using the similar strategy, Shi *et al.* developed light-driven PNIPAm-gold nanoparticles (AuNPs)/PAAm bimorphic hydrogel actuator by introducing AuNPs into PNIPAm hydrogel.[122] The resulting bimorphic soft actuators were found to show reversible motions and local hand-like finger flexion upon flood light illumination or local irradiation. Chen *et al.* reported light-driven PNIPAm-GO/GO bimorphic hydrogel actuator with GO acting as both a passive layer and a photothermal agent.[123] It has been reported that hydrogel actuators could self-fold into desirable shapes and change degrees of freedom in response to external stimuli through some complex and programmed design such as origami.[124,125] Zhu *et al.* demonstrated light-driven shape-programmable hydrogel actuators with zero Poisson's ratio by precise control of spatial arrangements of gold nanoparticles grafted with PNIPAm in between nonresponsive polymer stacks.[126] It should be noted that wavelength-selective light-driven programmable deformation of PNIPAm-based soft actuators could be faciely obtained through controlling the thicknesses of nonresponsive and responsive layers as well as introducing plasmonic nanoparticles with different shape and size such as gold nanoparticles and nanoshells (**Figure 10d, e**). These programmable soft actuators could promote the development of next generation “smart” soft robots, artificial muscles and beyond.

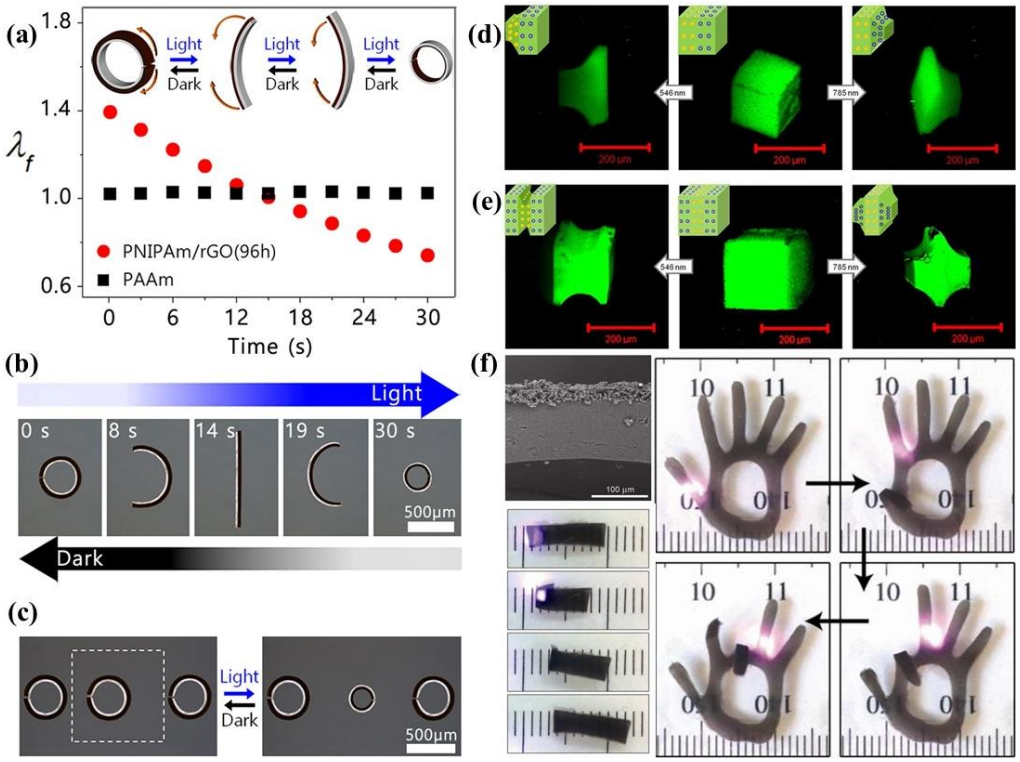

Figure 10. Hydrogel-based bimorphic soft actuators. a) Linear swelling ratio λ_f of PNIPAm/rGO and PAAm as a function of light irradiation time. b) Light-driven bidirectional bending of bimorphic hydrogel actuators. c) Selective light control of bimorphic hydrogel actuators. Reproduced with permission from ref. 120. Copyright© 2016, Nature Publishing Group. d, e) Wavelength-selective light-driven deformation of PNIPAm-based soft actuators. Reproduced with permission from ref. 126. Copyright© 2015, American Chemical Society. f) ELP-rGO bimorphic hydrogel actuators for light-driven soft crawler and "joint" bending of fingers on artifical hand. Reproduced with permission from ref. 127. Copyright© 2013, American Chemical Society.[127]

Besides PNIPAm, many other hydrogels such as elastin-like polypeptides (ELPs) could also exhibit hydrophilicity-hydrophobicity transition upon changing the temperature, and they are soluble below a transition temperature and above it they phase separate. Wang *et al.* demonstrated light-driven ELP-rGO bimorphic hydrogel actuators by cross-linking ELP-functionalized rGO into an ELP-based soft network anisotropically porous ELP-based hydrogels,[127] where diverse mechanical motions could be obtained through controlling the shape and surface patterns as well as modulating the positioning, timing and path of external light irradiations. For example, the authors developed hand-shaped soft actuator, and they could actuate the "joint" of fingers in any position and arbitrary order along each finger (**Figure 10f**). Although

great advances have been achieved in the development of light-driven hydrogel-based soft actuators, some critical issues or drawbacks need to be further adressed. The first one is slow response speed and long response time compared with other soft actuators, and three useful methods can be implemented: i) changing the molecular structure of hydrogel segment, for example, the comb-type grafted hydrogels could respond to environmental temperature faster;[128,129] ii) adjusting the LCST to a lower temperature;[130] iii) improving the photothermal conversion efficiency of photothermal agents[131] or using a higher laser power. The second one is low mechanical strength, which is one of huge barriers to the development of hydrogel-based soft actuators and their application in complex surroundings. To solve this problem, diverse methods have been proposed, such as nanocomposite gels[132], reinforcing by nanofibrillated cellulose[133] or cellulose nanocrystals.[9] It should be noted that although these reported methods could increase the mechanical strength and deswelling rate of hydrogels, some adverse effects could occur such as decreased strain, slow swelling rate, and small deformation degree.

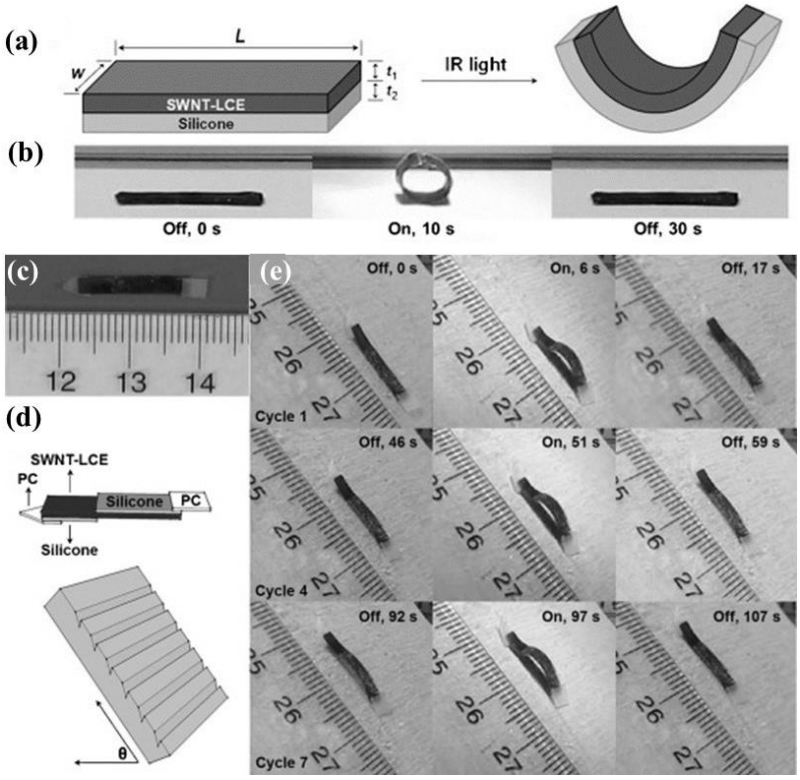

Figure 11. Light-driven SWNT-LCE/silicone bimorphic soft actuator. a) Schematic deformation of SWNT-LCE /silicone bimorphic soft actuator upon IR light irradiations. b) Photograph showing

deformation of bimorphic soft actuator when the IR light is turned on and off. c, e) Photograph showing light-driven LCEs-based soft crawler on d) a ratcheted substrate. Reproduced with permission from ref. 134. Copyright© 2013, Wiley-VCH.

Nematic-isotropic (N-I) phase transition is often observed in thermotropic liquid crystalline polymers (LCPs) such as liquid crystal elastomers (LCEs) and liquid crystal networks (LCNs).[11] Upon increasing the temperature, the aligned liquid crystal mesogenic units would become amorphously oriented, which are able to induce dramatic and reversible contraction (30-400%) along the direction of alignment.[135,136] Light-driven soft actuation could be faciely achieved through introducing various photothermal molecules or nanomaterials into thermotropic LCPs. By introducing CNT into LCE, the CNT-LCE composite films were reported to display a reversible and significant contraction in response to external light irradiations.[137-139] For example, Marshall *et al.* proposed that LCE-CNT artifical muscles with optimized CNT loading and superior alignment were able to provide the stroke of 10%, stress of several kPa and the response rate of a few seconds.[138] In spite of such an obvious contraction, the lack of a global bending motion seriously limits soft robotic applications of thermotropic LCEs. Taking advantage of silicone as a passive layer, Moua *et al.* fabricated IR light-driven hinges composed of SWNT-LCE composite/silicone bimorphic soft actuators (**Figure 11a**).[134] Upon IR irradiation, the significant in-plane negative strain of SWNT-LCE layer was constrained by silicone elastomer layer, resulting in SWNT-LCE layer bended the underlying silicone elastomer layer (**Figure 11b**). As walking devices, the IR light-driven inchworm-inspired walker based on SWNT-LCE/ silicone bimorphic soft actuators was able to crawl up a hill at a 50° incline with a walking velocity of 0.1 mms^{-1} in response to on/off cycles of IR light (**Figure 11c-e**). Interestingly, the directional movement of the device on a ratcheted substrate could be realized by the directional movement of IR light from the front to the center of the device and corresponding directional IR actuation. Inspired by unique feature of cuttlefsh skins, Chen *et al.* developed a light-driven smart bimorphic soft actuator that could simultaneously change surface color and shape-morphology under

infrared (IR) light irradiation.[140] To fabricate this bimorph soft actuator with unique structure color, the crosslinked polystyrene nanoparticles were assembled on the surface of PDMS to come into being elastomeric photonic crystal layer. Upon localized IR irradiation, the actuator layer was found to exhibit fast, large, and reversible strain in the irradiated region, leading to a synergistically coupled shape change in the laminated film and color change of the photonic crystal layer in the same region.

Besides CNT,[141] many other photothermal nanoagents with high light absorption and high photothermal conversion efficiency such as graphenes,[142,143] metal nanoparticles,[144,145] have been used as nanofillers in LCE-based soft actuators. For example, taking advantage of superior photothermal effect of gold nanorods (GNRs), Yang *et al.* developed GNR/LCE soft actuators that could shrink dramatically under 808 nm NIR light illumination,[144] which could lift up piece of capillary glass pipette with weight load (ca 3.0 mg) under NIR stimulus. However, there is an unambiguous problem involving the compatibility between LCEs matrix and photothermal agent, the doping concentrations of photothermal agents are limited, which restrict the photothermal effect and weaken the photoactuation speeds of the LCN actuators, thus surface modification of the inorganic nanofillers with appropriate (polymer) ligands are often needed.[146] On the other hand, the incorporation of nanofillers can dramatically improve the mechanical properties of LCEs and also affect its actuation behavior.[137] Therefore, many efforts have been devoted to fabricating LCE-based bimorphic soft actuators by integrating the photothermal nanoagents on the surface of LCEs.[147-149] For example, Dong *et al.* constructed soft actuators through simply packing thin RGO top layer and a LCN bottom layer together with an inactive polymer middle layer serving as connection adhesive.[144] Upon exposing the RGO side with a moving NIR light, a moving wave along the strip actuator was generated, which made the strip an effective caterpillar walker with unprecedented light-driven locomotion capability. Recently, Lan *et al.* reported a NIR photodriven polymeric oscillator by selectively coating a mussel-inspired polydopamine (PDA) polymer layer on the surface of splay-aligned liquid crystalline network (LCN) film.[148] It was found that the PDA-coated LCN soft

actuators could even exhibit fast and steady oscillation under focused sunlight, and a solar power generator was developed through transferring the solar energy into mechanical work and electricity. The unprecedented strategy of using solar light to drive polymeric oscillators is expected to provide new inspiration into the design and manufacture of advanced functional soft robotics and solar power generation devices.Interestingly, Zuo *et al.*[150] reported wavelength-selective light-driven bimorphic soft actuator through the modulation of light stimulus with three different wavelength bands (520, 808, 980 nm). The LCE-based bimorphic soft actuator was fabricated with a crossed angle of 45° between the alignment directions of two different LCE layers. Such a bimorph soft actuator could preform a right-handed helical twisting under 808 nm NIR light irradiation while excute a bending deformation under 980 nm NIR light irradiation. Overall, the fundamental mechanism behind these light-driven LCE-based soft actuators is the nematic-isotropic transition of LCEs, and the incorporation with a highly effective photothermal agent in LCEs could open new opportunity fot the development of bioinspired soft robitics toward their applications in diverse fields.[146]

In summary, we have introduced recent development of photothermal bimorphic soft actuators in this section. Photothermal actuation result from light-induced dynamic stress gradient and the subsequent shape change of bimorphic soft actuators, where the external light energy is converted into in situ heat through non-radiative thermal relaxation processes of organic dyes or functional nanoparticles. Photothermal expansion and photothermal contraction or shrinkage are two dominating mechanisms for light-driven bimorphic soft actuators as summarized in **Table 2**. Bimorphic soft actuators based on photothermal expansion are generally developed by combing two layers with different CTEs, where photothermal agents could function either as part of photoactive layer or directly as photoactive layer. Bimorphic soft actuators based on photothermal expansion often involve the materials with negative CTE such as hydrogels, graphene derivatives and liquid crystals, the mechanism of photothermal contraction mainly includes photothermal desorption of water molecules and

photothermally indeced different phase transitions such as metal-insulator transition, hydrophilicity-hydrophobicity transition and nematic-isotropic transition. Although visible light-driven systems have been demonstrated, photothermal bimorphic soft actuators are mostly powered by near-infrared light due to the higher photothermal conversion efficiency in near-infrared regions, which could open new door for developing sunlight-driven bimorphic soft actuators since more than 50% of solar radiations arrives at the earth in the form of near-infrared light. It should be also noted that actuating performances of bimorphic soft actuators are closely related to their overall thickness and the choice of photothermal agents and soft materials with large CET difference. Photothermal actuating strategies are expected play increasingly important roles in the development of light-fuelled soft robotics with rapid actuation.

Table 2. Mechanisms, materials, actuating performance of representative photothermal bimorphic soft actuators.

Mechanism		Materials	Thickness d [μm]	Light intensity P [mW cm^{-2}]	Time t [s]	ΔT [°C]	Curvature κ[cm^{-1}]	Ref.
Photothermal volume expansion		PI/paraffinwax/CNT	33	100 (Vis)	0.87	20	0.74	34
		PDMS/PDMS-GNPs	130	2950 (NIR)	5	60	0.4	77
		PDMS/RGO-CNT	120	250 (Vis)	3.6	80	0.35	92
		PC/CNT	11	100 (Vis)	0.87	25	0.63	89
		PMMA/AuNRs-RGO	25	50(IR)	0. 5	35	2.0	91
Photothermal volume contraction	Photothermal desorption	BOPP/graphite/paper	67	300 (NIR)	10	41.4	1.9	46
		PC/MXene-cellulose	20	80 (NIR)	6.6	54.5	0.84	63
		PDA-rGO/NOA-63	10	22 (NIR)	2	-	0.96	64
		GO/EC	40	140 (NIR)	10.3	25	2.0	102
	Metal-insulator transition	VO_2/SWCNT	0.92	38000 (Vis)	0.008	68	2.2	115
		W-VO_2/CNT	1.68	800 (Vis)	0.029	34	4.4	116
		PNIPAm-AuNPs/PAAm	235	150 (Vis)	24	-	4.28	122

Hydrophilicity-hydrophobicity transition	g-PNIPAm-MNP/PAAM	50	41.8 (Vis)	60	-	75	128
	GO/GO- PNIPAm	-	200 W (NIR)	90	25	2.2	123
Nematic-isotropic transition	LCE- SWNTs/ silicone	400	1160 (NIR)	10	68	2.8	134
	LCE- dyes /LCE	500	180 (NIR)	32	47	3.2	150
	LCE-SWNTS	275	4500 (NIR)	15	55	2.8	140

4. Photochemical Bimorphic Soft Actuators

Photochemical soft actuation that couples remote light and chemical molecular reactions to power and control mechanical motion, is another class of smart actuation principle with great potential. It should be noted that the sun-tracking leaf of Cornish Mallow plant is a typical example of such an advanced photochemical actuation system in nature, where the plant is thought to use a combination of chemical light receptors and signal transmitting compounds to controll movement of the leaf and face the moving sun throughout the day.[151,152] Many different photochromic materials such as spiropyran, diarylethenes and azobenzene derivatives that exhibit reversible photochemical reactions upon light irradiations have been utilized to develop light-driven soft actuators, robotics or machines.[153-156] Liquid crystal polymers (LCPs) with ordered nanostructures are known to exhibit unprecedented advantages and great potentials in the development of light-fuelled soft robotics thanks to their fascinating features such as entropic elasticity of polymeric elastomers and photodeformable ability upon the introduction of photochemical molecules.[157] Herein, we mainly focuse on the recent advances in the development of photochemical bimorphic soft actuators that are achieved by introducing photoresponsive azobenzene into the active layer based on anisotropic soft matter matrix of liquid crystalline polymers (LCPs), where light-driven dynamic geometrical changes of azobenzene molecules can be autonomously amplified into macroscopic and reversible shape deformation deformation such as bending and curling under the external light irradiations. Moreover, we also introduce the

development of bimorphic liquid crystalline actuators combined with both photochemical and photothermal actuation.

4.1 Azobenzene-based bimorphic liquid crystalline actuators

Light-driven reversible deformation of azobenzene-based liquid crystalline actuators is usually induced by the configuration change of azobenzene and orientation variation of LC molecules, which can be subsequently amplified into a macroscopic deformation of soft actuators. It is well-known that two reversible isomeric states are often observed in azobenzenes upon light irradiation at an appropriate wavelength: a rod-like trans isomer that stabilizes the structure of LC phase and a bent-shape cis isomer that tends to destabilize the LC phase. It should be noted that photothermal effect was also observed in azobenzene derivatives,[23] and azobenzenes could also exhibit some special photochemical properties such as photoreorientation upon polarized light irradiation.[158-160] Taking advantages of photoinduced phase transition in azobenzene-doped LCs, the introduction of azobenzene units into LCP-based freestanding crosslinked films with different molecular alignment have been demonstrated to facilitate a variety of light-driven fast and reversible macroscale mechanical actuations such as bending, twisting and buckling.[161] Interestingly, light-driven bimorphic soft actuators that combine a photoactive LC layer with a passive layer were found to endow soft actuators with unprecedented features such as ultrasensitivity, programmability, superior compatibility, robust functionality and easy controllability. For example, Ikeda *et al.* pioneered a novel sophisticated light-driven plastic motor based on azobenzene-doped bimorphic liquid crystalline actuators.[162] LCE films with Azobenzene in crosslinker were firstly fabricated through photopolymerizing the LC mixture in a glass cell coated with rubbed polyimide alignment layers, and bimorphic soft actuators were subsequently developed by laminating the photoactive LCE layer and a flexible low-density polyethylene (LDPE) film together. A plastic belt of such LCE bimiorphic film could be achieved by connecting both ends of the film, and then placed the belt on a homemade pulley system. Interestingly, the belt was able to rotate and drive the two

pulleys in a counterclockwise direction upon irradiating with UV light from top right and visible light from top left simultaneously. It is worth noting that the opposite rotation of this motor can be faciely realized by simply exchanging the irradiation positions of the UV and visible light. The light-driven plastic motor could efficiently convert external light energy into mechanical force without any gears, batteries and electric wires, which paves new way for the development of noncontact and battery-free advanced soft robotics. Moreover, Yu *et al.* reported light-driven bimiorphic cantilever soft actuators by coating azobenzene-based photoactive liquid crystalline polymer on a LDPE substrate with microgroove structures acting as the alignment layers.[163] Upon solvent evaporation and thermal annealing, a bimorphic soft actuator could be obtained with homogeneously aligned mesogens along the groove direction. An optical pendulum generator was developed for converting light energy into electricity through attaching copper coils onto one free end of as-prepared bimiorphic cantilever soft actuator. Upon UV-irradiating the soft acturators, a continuous and self-sustained oscillation could be achieved thanks to the light-driven cantilever swing motion from alternative exposure and shielding light upon the bimorphic soft actuators, which was used as an optical pendulum generator for producing an alternating voltage under a magnetic field and continuous external light irradiations. It was found that the light-driven output electricity was proportional to the changing rate of the magnetic flux and was closely related to many parameters such as light intensity and film thickness. The strategy disclosed herein could provide important insights into the development of light-fueled soft actuators toward solar harvesting and energy storage applications.

Zhao *et al.* developed light-driven moving wheels and spring-like motors based on bimorphic soft actuators (**Figure 12**).[74] They designed and synthesized a azobenzene-containing liquid crystalline elastomers (LCEs) through the catalytic transesterification reaction, and the resulting highly stretched LCE film was laminated with a flexible and biaxially oriented polypropylene film (BOPP, 45 μm in thickness) to fabricate the light-driven bimorphic soft actuators. The bimorphic film was cut into rectangular stripe (85

mm × 8.5 mm) and then rolled into wheel with closed tubular shape. When LCEs film acted as the outer layer of the wheel, the nonuniform bending of the LCE outer layer upon UV light irradiation resulted in the curvature decrease of the bimorphic actuators on the light-facing side. As shown in **Figure 12a**, the right side receiving illumination tended to be flatten while the unexposed left side kept unchanged. Such asymmetric photoinduced deformation led to a shift of the center of mass to the left side, thus resulting in a torque that could drive the wheel rolling away from the light source on a flat surface (**Figure 12c**). Interestingly, the wheel rolling direction could be easily reversed toward the light source through seting the stretched LCE film as the inner layer (**Figure 12b**). When the UV irradiation passed through the BOPP outer layer, the bending of the inner LCE layer would increase the curvature of bimorphic soft actuators instead of flattening the outer layer, while the left part of the wheel kept unchanged. As a result, this asymmetric deformation led to a shift of the wheel's center of mass to the right side, thereby leading to a torque that drives the wheel rolling toward the light (**Figure 12d**). The authors also demonstrated light-driven spring-like motors using as-prepared BOPP/LCEs bimorphic soft actuators, where light could be faciely transferred into mechanical energy to execute a variety of tunable, robust, and continuous motions at the macroscopic scale. It was found that both wheels and spring-like motors could roll away from or toward the UV light by setting the stretched LCE film as the inner or outer layer, and the rolling speed could be easily controlled by adjusting the amount of stored energy in the LCE film with different elongation degrees. The strategy of prestoring a controllable amount of strain energy to obtain a strong and tunable photoinduced mechanical force in bimorphic soft actuators is anticipated to pave newway for the development of light-driven soft robotics.

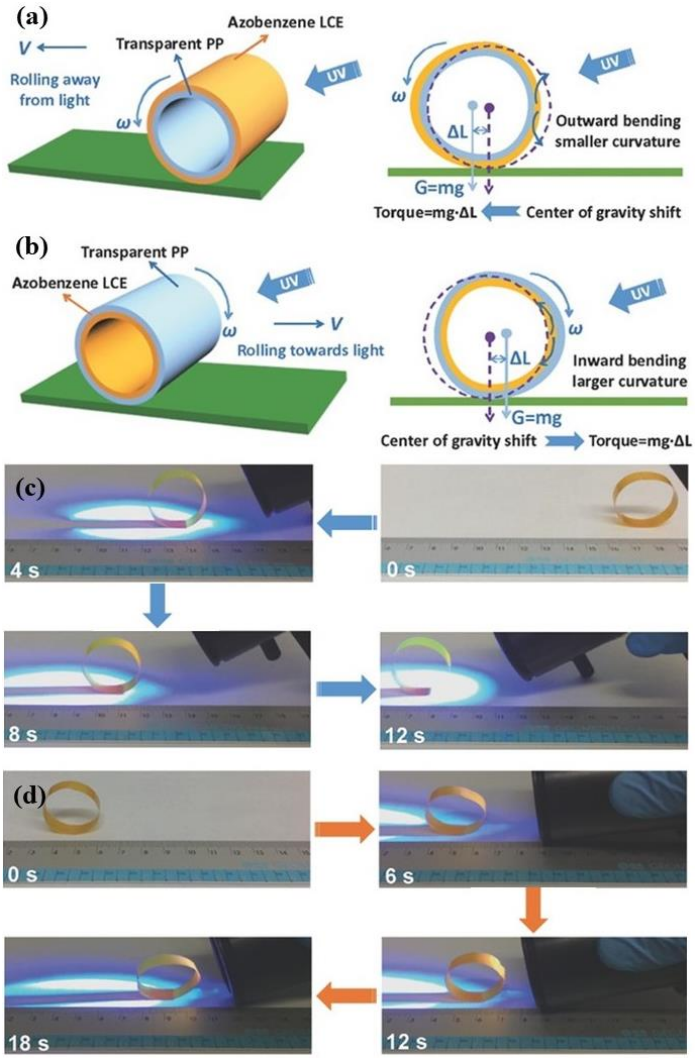

Figure 12. Light-driven moving wheels based on bimorphic soft actuators. Scheme showing the mechanism of a) rolling away from or b) rolling toward the light source. Photographs showing continuous light-driven forward rolling wheels with LCE film set as the outer layer c), and d) backward rolling wheel with LCE film set as the inner layer. Reproduced with permission from ref. 74. Copyright© 2017, Wiley-VCH.

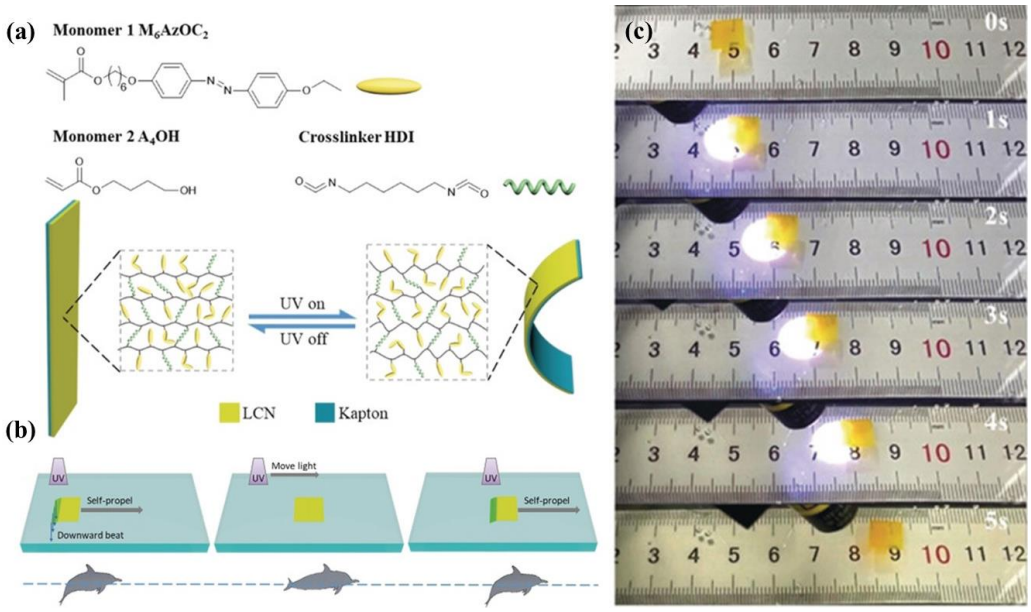

Figure 13. Light-driven artifical swimmers based bimorphic soft actuators. a) Schematic illustration of photoinduced bending based on LCPs/PI bimorphic soft actuators. b, c) Schematic swimming mechanism images of bioinspired artifical swimmer propelled by UV irradiation. Reproduced with permission from ref. 166. Copyright© 2019, Wiley-VCH.

Homogeneously aligned LCE films with azobenzene in crosslinker are known to exhibit shape contraction upon UV light irradiation due to photoinduced reduction of mesogenic ordering. In contrast, a light-driven shape expansion could be observed in homogeneously aligned LCE films with azobenzene in the side chain of the cross-linked LC network since photoisomerization process of azobenzene is decoupled from the LC network.[164] Researchers have made some efforts to develop light-driven bimorphic soft actuators based on LCE films with azobenzene in the side-chain.[160,161] For example, Hagaman *el at.* developed light-driven bimorphic soft actuators via 3D printing poly(siloxane) LCs with pendant azobenzene groups onto of commercially available Kapton polyimide thin films.[165] Upon UV light irradiation, a gradient stress between the active and passive layers was generated through photoinduced volume expansion from the trans-cis isomerization of azobenzene, as a result the as-prepared bimorphic soft actuators were found to exhibit rapid and reversible actuation with full cycles completed on the time scale of seconds. Yu *et al.* demonstrated light-driven bimorphic soft actuators for bioinspired artificial swimmers that exhibit fast,

continuous, and on-demand remote controlled motion at liquid/air interfaces.[166] The bimorphic soft actuators were fabricated through coating liquid-crystalline polymer film (7.3 um) with azobenzene in the side-chain onto a commercially available Kapton polyimide substrate (14.8 um). Upon UV light irradiations, photoinduced volume expansion resulted in a distinctive bending direction towards the polyimide side, and the bimorphic film would immediately returned to its original shape in about 2 seconds as shown in **Figure 13a**, where the bending and unbending deformations were believed to result from the generation and elimination of UV light-induced stress between the active and passive layers. Interestingly, light-driven artificial swimmers based as-prepared bimorphic soft actuators were found to exhibit continuous forward motion away from the light source on the surface of ethanol/water (50% volume ratio), and the motion would stop immediately upon removal of light irradiations. The authors elaborated the motion mechanism of artificial swimmer as the "dolphin kick" style. The artificial swimmer film kept still and flat when placed on a liquid surface with the Kapton side facing the liquid interface. Upon UV irradiating the left part, the film would bend downward and beat the liquid like a dolphin fluttering its tail fin, and in turn the liquid pushed backward and propel the swimmer forward (**Figure 13b, c**). It is worth noting that the recovery process of the deformed film on the liquid surface should be greatly accelerated compared to that in air because of the reactive force from the displaced liquid. Importantly, the authors demonstrate the on-demand directional control over artificial swimmers, and both the forward movement and rotation motion were achieved by mimicking the motion of a dolphin. The light-driven artificial swimmers based bimorphic soft actuators could open a new door for the development of bioinspired soft robotics toward diverse applications such as light-controllable transportation, underwater task and beyond.

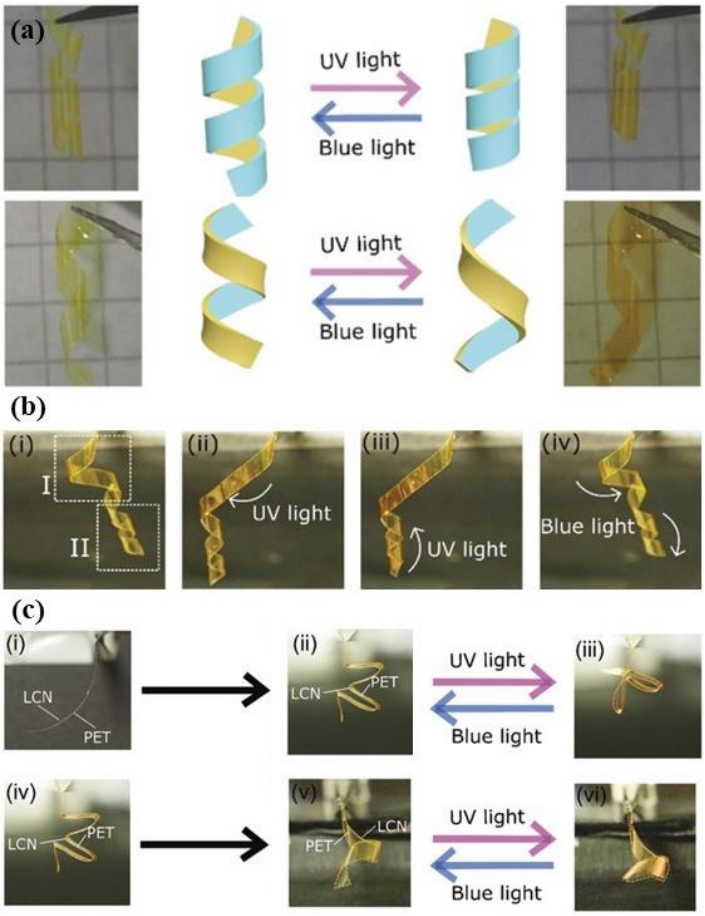

Figure 14. Reprogramming light-driven bimorphic soft actuators. a) Light-driven spiral actuators with LCP layer on the inside and outside of the helix, respectively. b) Light-driven dual-mode soft actuators composed of two sections with LCN outside and inside, respectively. c) shape programming/re-programming and light-driven complex shape morphing in a single soft actuator. Reproduced with permission from ref. 169. Copyright© 2020, Wiley-VCH.

To develop light-driven bimorphic soft actuators with programmable attributes, Zhao *et al.* fabricated a novel main-chain liquid crystalline Diels-Alder dynamic networks (LCDANs), and bimorphic soft actuators were fabricated through laminating a monodomain LCDAN strip with a flexible Kapton polyimide film.[168] It shoud be noted that such bimorphic soft actuator could be facilely programmed into any desired shape due to the excellent programming and reprocessing properties of LCDAN. For example, the bimorphic soft actuator was shaped into a light-driven caterpillar-inspired arching walker. With the two ends well-designed for unbalanced friction with the substrate surface, the walker could crawl forward upon repeated UV light on/off cycles. The bimorphic soft actuator could be also programmed into a light-driven rotating

wheel. Upon UV-light illumination, the curvature of the light exposured side was found to decrease so that bending toward the outer LCDAN layer, the resulting asymmetric curvature change would drive the wheel rolling away from the light beam. Schenning *et al.* demonstrated reprogrammable light-driven bimorphic soft actuators with arbitrary initial shapes through spray-coating of polyethylene terephthalate (PET) with an azobenzene-doped liquid crystalline polymers, where PET played an important role in increasing the ductility and aligning mesogens of the spray-coated liquid crystalline polymers.[169] Shape programming and shape morphing are achieved by using different stimuli. Thermally shaping and fixing the thermoplastic PET allows arbitrary configurations such as origami-like folds and different handed helicity, and the thermally fixed geometries can be reversibly actuated upon light exposure, with fast and reversible area-specific actuation such as winding, unwinding and unfolding. By this method, two identical helical actuators could be made to actuate in contrasting manners (**Figure 14a**), which were coated photoactive LCPs on the inside or the outside, resulting in helix winding and helix unwinding upon UV light illumination, respectively. It should be noted that opposing actuation modes within a single sample could be achieved through integrating two opposite helical twisted structures into the same bimorphic soft actuators, where multiple intermediately shaped morphing configurations were possible (**Figure 14b**). Interestingly, the authors also demonstrated light-driven accordion-like bimorphic soft actuators that simultaneously exhibited complex actuation behaviors such as origami-like bending and spiral helical unwinding (**Figure 14c**). The strategy disclosed herein is expecte open numerous possibilities for developing bimorphic soft actuators toward programming and reconfigurable soft robotics.

Yu *et al.* reported red light-driven bimorphic soft actuators by laminating dual-dye upconversion polyurethane onto azobenzene-containing LCEs (**Figure 15a**).[170] The dual-dye upconversion system was based on highly effective red-to-blue triplet-triplet annihilation (TTA), the upconversion polyurethane film was developed through codoping a Pt(II) complex tetraphenyltetrabenzoporphyrin (PtTPBP) sensitizer with a

9,10-bis(diphenylphosphoryl)anthracene (BDPPA) fluorescent dye (**Figure 15b**). Under 635 nm laser excitation, the PtTPBP&BDPPA-containing polyurethane layer was found to generate the intense blue emission that matched well with a strong absorption band of azotolane-containing liquid crystalline layer, resulting the bending of bimorphic soft actuators toward the light source along the alignment direction of the mesogens (**Figure 15c, d**). The upconversion polyurethane layer could upconvert 635 nm irradiation light into the blue emission that was then absorbed by the azotolane moieties in LCE layers via the emission-reabsorption process, thus inducing the trans-cis photoisomerization and the subsequent shape deformation. Photoinduced bending toward the light source were believed to result from gradient adsorption of blue light across the LCE film and light-driven contraction at its front surface region. Interestingly, it was found that polyurethane played an important role in achieving light-driven bimorphic soft actuators, and the LCEs coated with only PtTPBP&BDPPA powder exhibited no bending behavior upon red light irradiation at 635 nm. The strategy disclosed herein is expected to provide new insights into the development of long-wavelength light-driven soft robotics with advanced upconversion nanotechnology.

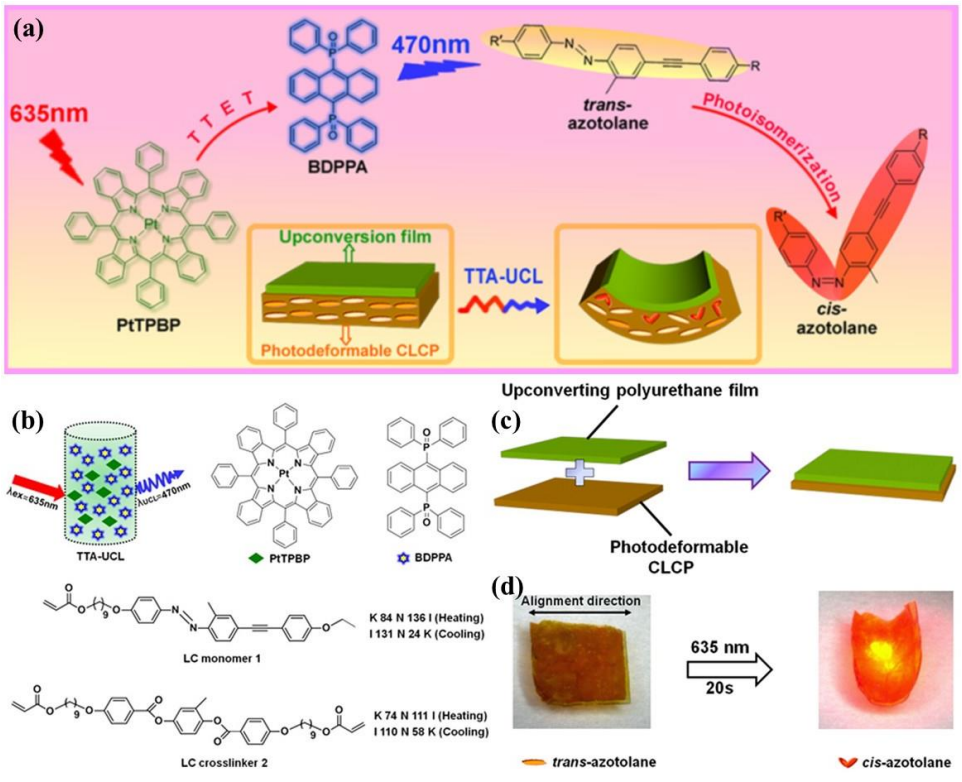

Figure 15. Red light-driven bimorphic soft actuators based on upconversion technology. a) Schematic mechanism of upconversion-based light-driven bimorphic soft actuators. b) Illustration of PtTPBP (sensitizer), BDPPA (annihilator) and upconversion emmision upon 635 nm excitation, LC monomer and crosslinker. c) Schematic fabrication of upconversion-based bimorphic soft actuators. c) Image of red light-driven actuation of bimorphic soft actuators. Reproduced with permission from ref. 170. Copyright© 2013, American Chemical Society.

4.2 Bimorphic soft actuators with synergistic photochemical and photothermal effects

Photochemical and photothermal effects can be used simultaneously to realize light-driven bimorphic liquid crystalline actuators, and both mechanisms have their own strengths.[171,171] For photochemical actuation, the photochemical molecules such as azobenzenes are preferably required to be covalently bonded within liquid crystalline polymer network. Cis-trans isomerization of typical azobenzenes are usually photoactivated upon irradiation within the 450–550 nm range, and the long-life time of cis-isomer often leads to a relatively slow actuation speed of several seconds or even minutes. For photothermal actuation, photothermal agents can be easily doped into the liquid crystalline polymer network to generate efficient photoactuation upon light irradiation with different wavlengths ranging from the visible to the NIR. It is worth noting that photothermal actuators are able to deform rapidly, within milliseconds to seconds, depending on the heat capacity. Therefore, A combination of two different photoactuation mechanisms in one single actuator should enable robust, programmble and reconfigurable soft photoactuators that could respond to multiple wavelengths independently and execute sophisticated motion tasks upon simultaneous photochemical and photothermal actuation in one device.[32,173] The “actuation on command” could be expected in light-driven bimorphic soft actuators through synergistic use of photochemical and photothermal effects.

Zhao *et al.* reported a general approach to develop both NIR and UV light-driven soft actuators with enhanced photoactuations by integrating polymer-grafted gold nanorods (AuNRs) with dynamic azobenzene-containing liquid-crystalline networks (ALCN).[174] Interestingly, AuNR-ALCN films with stretched alignment were found to

exhibit two different actuation behaviors powered by UV-Vis and NIR light, respectively. Upon UV light irradiation, AuNR-ALCN film underwent bending motions and kept the bending state unless exposure to visible light to decrease the remaining stress. In contrast, AuNR-ALCN film displayed reversible bending and unbending motions just by turning on and off the NIR light (**Figure 16a**). The UV light-driven contraction force was believed to originate from both trans-cis photoisomerization of azobenzene and photothermally induced polymer chain relaxation, and such contraction force would not drop completely upon turning off the UV irradiation because of the remaining cis state of azobenzene that could diminish through visible light irradiation. Besides, the NIR light-driven actuation force was found to only depend on the shape contraction when heated above its LC phase transition temperature, and such light-driven reversible shape change could be easily achieved just by turning on and off NIR irradiations. Importantly, the authors developed light-driven bimorphic soft actuators that could execute programmable, localized, and specified motion tasks by laminating a stretched AuNR-ALCN layer with a commercially available transparent biaxially oriented polypropylene film (BOPP, $\approx$ 45 μm in thickness). The as-prepared bimorphic soft actuators were found to exhibit different UV-light-driven bending downward or upward directions with the AuNR-ALCN layer set as bottom layer or top layer, respectively (**Figure 16b**). The authors demonstrated a variety of versatile and complex motions based on bimorphic soft actuators, for example, light-driven caterpillar-inspired walker that can crawl forward on a ratcheted substrate, and photocontrolled plastic "athletes" that could do push-ups and sit-ups through locally programming the alignment of AuNR-ALCN layer in the athlete's arms and waist, respectively (**Figure 16c**). Moreover, the authors proposed the concept of light-driven artifical crane that could perform distinct photomechanical functions including grasping, lifting up, lowering down, and releasing an object, based on the synergistic photomechanical effects of photochemically driven trans–cis photoisomerization and photothermally induced liquid-crystalline–isotropic phase transition. As shown in **Figure 16d**, the gripper could grasp and firmly hold the tubular-

shape object upon UV light irradiation, and the telescopic arm would lift up the object upon NIR illumination thanks to a rapid contraction in length resulting from the photothermally induced LC–isotropic phase transition, and the telescopic arm would return to its original state and the gripper would liberate the object upon removal of the NIR and UV light in sequence. Such light-driven bimorphic soft actuators based on synergistic photochemical and photothermal effects open numerous possibilities for the development of truly advanced, biomimetic and intelligent soft robotics.

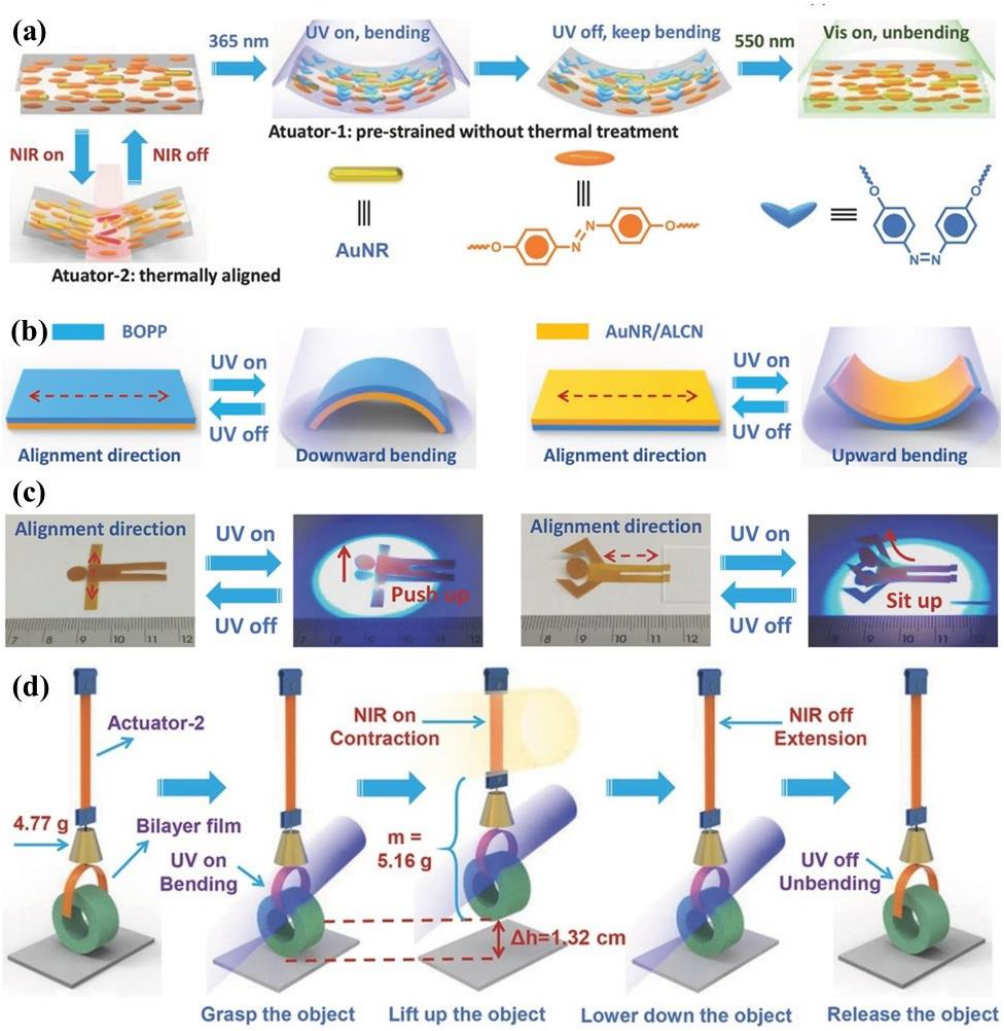

Figure 16. Light-driven bimorphic soft actuators through synergistic use of photochemical azobenzene and photothermal gold nanorods. a) Schematic showing photothermal and photochemical mechanisms for different bending behaviors driven by NIR and UV-vis light, respectively. b) Schematic illustration of light-driven bending downward and upward with the AuNR-ALCN layer set as bottom layer or top layer, respectively. c) The images of light-driven plastic "athletes" that could push up and sit up. d) Schematic illustration of light-driven artifical "crane" that can execute a series of robot-like motion tasks. Reproduced with permission from ref. 174. Copyright© 2018, Wiley-VCH.

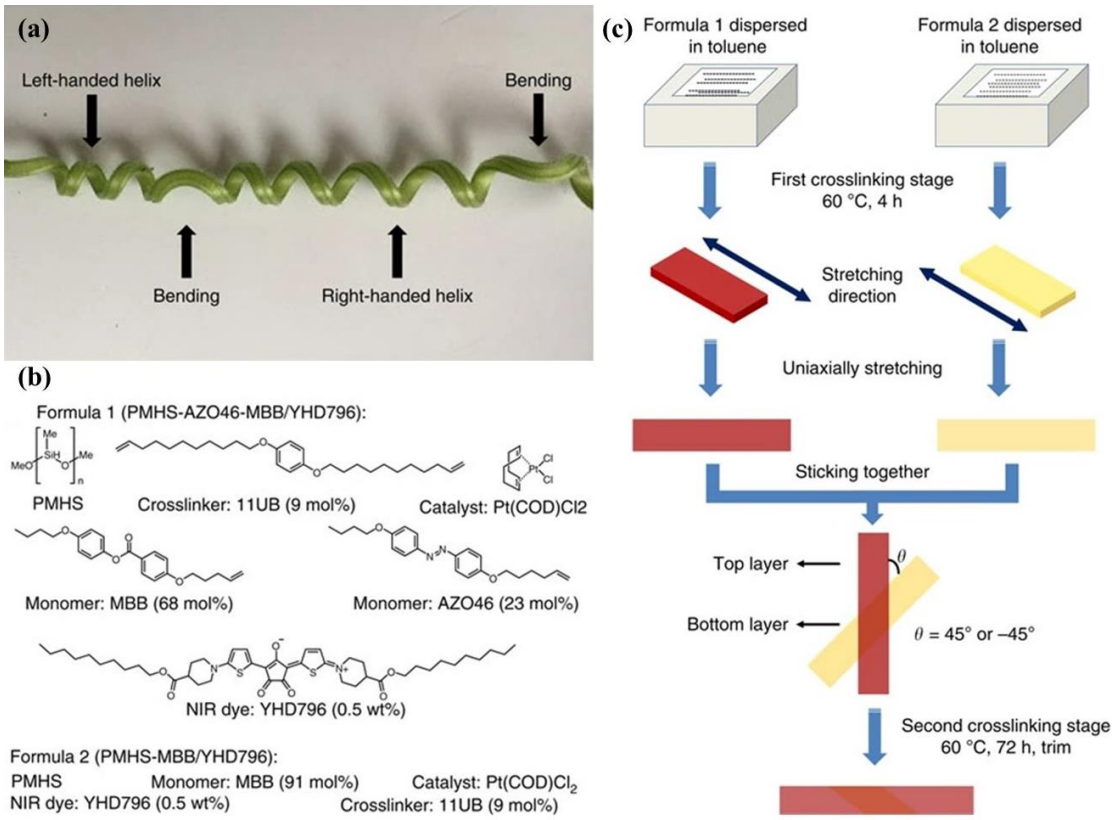

Figure 17. UV and NIR light-riven polysiloxane-based bimorphic liquid crystalline actuators. a) Bending and chiral twisting in plant tendril of cucumbers. b) The chemical compositions of top layer (Formula 1) and bottom layer (Formula 2) of bimorphic liquid crystalline actuators. c) Schematic illustration of fabricating light-driven bimorphic liquid crystalline actuators. Reproduced with permission from ref. 175. Copyright© 2016, Nature Publishing Group.

Inspired by plant tendrils in nature, Yang *et al.* demonstrated light-driven bimorphic soft actuators exhibiting wavelength-selective photoinduced 3D deformations (bending and chiral twisting) through the combination of photochemical azobenzene with organic photothermal dye in polysiloxane-based LCEs (**Figure 17a**).[175] In the bimorphic soft actuators, the top layer was made of a uniaxially aligned LCEs loaded with a azobenzene chromophore and a NIR absorbing dye, which would exhibit bending upon UV irradiation and shrinking upon NIR irradiation due the cis–trans isomerization of azobenzene and the photothermal heating LC-toisotropic phase transition from NIR absorbing dye, respectively. In contrast, the bottom layer was composed of LCEs doped with only NIR absorbing dye, which can only respond to external NIR irradiations (**Figure 17b**). The two layers were obliquely glued together,

and the different overlapped angles between the bottom and top layers (45 ^{o} or -45 ^{o}) could lead to a left-handed or right-handed helical curling upon light irradiations (**Figure 17c**). Interestingly, it was found that resulting bimorphic soft actuators exhibited similar bending behaviors toward the light upon UV irradiation, while right-handed or left-handed twisting actuation upon NIR irradiation that was dependent on overlapped angles between the bottom and top layers. The strategy disclosed herein is expected to offer new inspirations for the development of next-generation light-driven soft actuators that could perform diverse 3D motions according to the external light with different wavelengths, which could find important applications in areas of soft machines, biomimetic devices and beyond.

In summary, we have introduced recent development of photochemical bimorphic soft actuators with an emphasis on introducing photoresponsive azobenzene molecules into the active layer based on anisotropic liquid crystalline systems as summarized in **Table 3**. Azobenzene molecules could either be covalently crosslinked into the main chain of liquid crystalline polymer network or be bonded in the side chain of the cross-linked polymer network. Interestingly, homogeneously aligned LCE films with azobenzene in crosslinker are found to exhibit shape contraction upon UV light irradiation due to photoinduced reduction of mesogenic ordering. In contrast, a light-driven shape expansion was observed in homogeneously aligned LCE films with azobenzene in the side chain of the cross-linked LC network since photoisomerization process of azobenzene is decoupled from the LC network. Most Azobenzene-based bimorphic liquid crystalline actuators are reversibly driven by the alternating irradiations of UV and visible light, although near-infrared light-driven systems have been realized through optical upconversion strategies. It is worth noting that “actuation on command” was achieved in light-driven bimorphic soft actuators through synergistic use of photochemical and photothermal effects, where a combination of two different photoactuation mechanisms in one single actuator is expected to enable robust, programmble and reconfigurable soft photoactuators that could respond to multiple

wavelengths independently and execute sophisticated motion tasks upon simultaneous photochemical and photothermal actuation in one device.

Table 3. Mechanisms, materials, actuating performance of representative photochemical bimorphic soft actuators.

Mechanism	Materials	Thickness d [μm]	Light intensity P [mW cm^{-2}]	Time t [s]	Photoinduced force [mN]	Displacement [mm]	Ref.
Photochemical	LCN/PI	22.1	150 (UV)	2.4	55	23	166
	LCE/PE	65	240 (UV)	60	130	-	162
	LCN/PET	16	170 (UV) & 300 (Blue)	15	-	18	169
	PLAZ/LDPE	25	270 (UV)	5	180.1	-	167
	LCP/PI	20	100 (UV)	5	72	-	72
	Materials	Thickness d [μm]	Light intensity P [mW cm^{-2}]	Time t [s]	ΔT [°C]	Stress [MPa]	Ref.
Photochemical and Photothermal	GO/ALCN	120	700 (NIR)	15	54	1.35	32
			70 (UV)	15	47.6	0.74	
		150	6700 (NIR)	40	150	3	
	AuNR-ALCNs/BOPP	20	100 (UV)	30	-	8	174
		20	20 (Vis)	30	-	0	

5. Conclusion and Perspective

In this review, we provide a state-of-the-art advancement of light-driven bimorphic soft actuators, actuation mechanism and emerging applications, where the combination of a photoactive layer with a passive layer in one single bilayered system is believed to enable a large mismatch between both layers, and could endow soft actuators with unprecedented features such as ultrasensitivity, programmability, superior compatibility, robust functionality, easy controllability and superior actuating performance (**Figure 18**). Compared with bimorphic soft actuators powered by other stimuli such as the pneumatic, humidity, electric and magnetic fields, light-fueled smart

systems could be one of best candidates for the development of untethered, programmable and reconfigurable soft robotics thanks to their superior optical-to-mechanical energy conversion capacity and unique features of remote, spatial and temporal controllability. Light as an inexhaustible and sustainable energy source is ubiquitous in our dailylife, more than 50% of solar radiations arrives at the earth in the form of near-infrared light, and its physical parameters including intensity, wavelength, and polarization can be facilely tailored with high spatial and temporal resolution. In light-driven bimorphic soft actuators, the active layer basically dominates the volume change whether it expands or shrinks, and large volume change is often restricted by its mismatch with passive layer, thus resulting in benting deformation in response to external light irradiations. Light energy could be converted into thermal or chemical energy toward photomechanical deformation, and the corresponding actuation mechanisms are based on photothermal or photochemical effects. To fabricate light-driven bimorphic soft actuation, one must incorporate photoactive agents such as photothermal nanotransducers (nanoparticles or organic dyes) or molecular photoswitches (e.g. azobenzenes) into into soft matter matrix. These photoactive agents can serve to absorb the external light irradiations and facilitate photomechanical actuation through diverse optical processes such as photothermal expansion, photothermal desorption, photothermal phase transition, photochemical configuration changes and beyond. A variety of photothermal bimorphic soft actuators has been developed according to different expansion/contraction actuating principles such as photothermal-induced expansion, photothermal-induced desorption and photothermal-induced phase transition. Besides abundance in selection of photoactive and passive materials, the physical parameters of soft materials such as Young's modulus and CTE of different layers could be easily customized on-demand, for example, the anisotropy of bimorphic soft actuators could be facilely achieved by introducing anisotropic nanomaterials into appropriate layers, and sophisticated control over the anisotropy direction could generate a wide variety of shape deformations and bioinspired motions such as bending, spiral, twisting, and oscillation. Photochemical bimorphic soft

actuators could be fabricated by introducing photoresponsive azobenzene into the active layer based on anisotropic soft matter matrix of liquid crystalline polymers, where light-driven dynamic geometrical changes of azobenzene molecules can be autonomously amplified into macroscopic and reversible shape deformation deformation such as bending and curling under the external light irradiations. Moreover, light-driven bimorphic soft actuators could also be developed by the synergistic use of photochemical and photothermal actuations. Undoubtedly, light-driven bimorphic soft actuators can open up numerous exciting possibilities for developing bioinspired soft robotics with programmable and reconfigurable functions toward diverse applications ranging from artificial muscles to biomedical technologies and beyond.

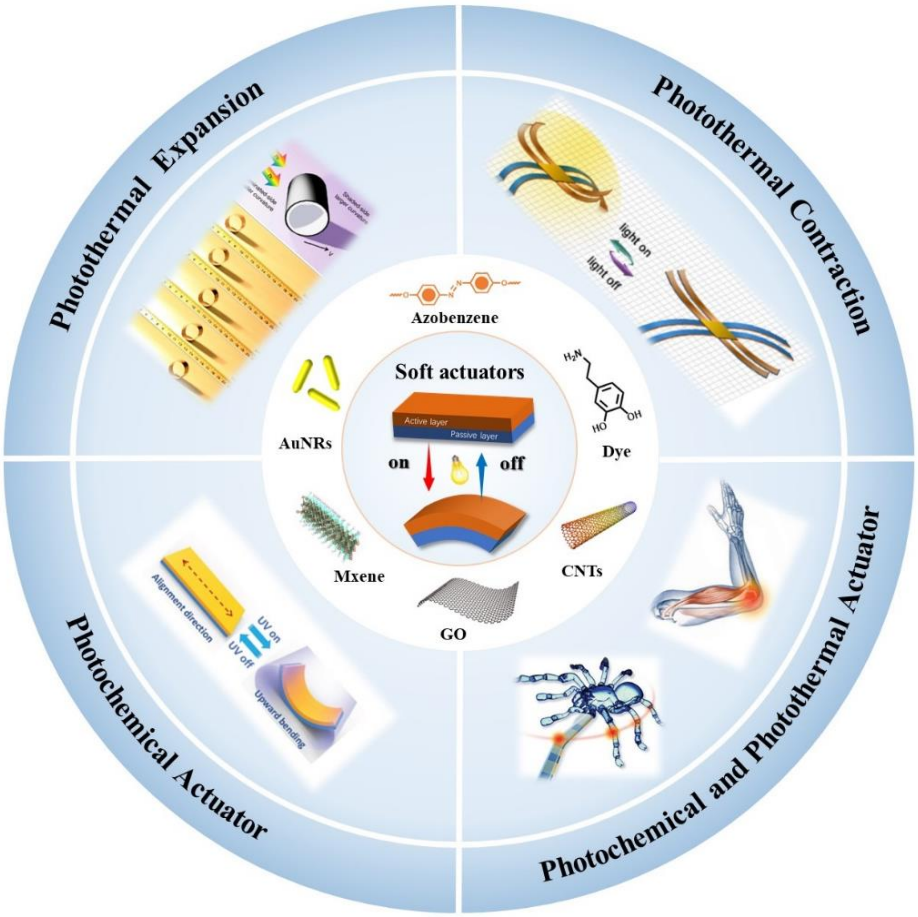

Figure 18. Schematic illustration of light-driven bimorphic soft actuators and emerging applications.

Although extensive advancements have been achieved in the design and fabrication of light-driven bimorphic soft actuators, the overall development is still in a very preliminary stage with many challenges and critical issues that need to be addressed. Compared with soft actuators based on homogenous and gradient structures, there is a risk of delamination taking place at the interface between both layers of bimorphic soft actuators, exploring new strategies to obtain the stable and robust interface is a prerequisite for developing light-driven bimorphic soft actuators with superior performance. For photothermal bimorphic soft actuators, an excellent photothermal agent should meet the following requirements: high photothermal conversion efficiency to ensure an efficient photothermal actuation, broad photoabsorption covering the full solar spectrum range toward sunglight actuation, superior compatibility with soft matter matrix as well as synthetic simplicity, good photostability and low cost. For photochemical bimorphic soft actuators, researchers mainly focused on introducing photoswitchable azobenzene molecules into anisotropic liquid crystalline matrix, more attentions should also be paid to many other promising soft matter matrix systems and photochromic materials such as spiropyran and diarylethenes. Moreover, infinite golden opportunities may be still hidden in the future research of light-driven bimorphic soft actuators. Taking advantage of unique bimorphic structure, soft actuators could be integrated many emerging advanced functional materials such as photonic coatings with bioinspired camouflage capability,[176] 2D/3D nanostructures with promising functions of signal detection and electromagnetic shielding,[177,178] as well as electronic skins and flexible integrated devices with self-feedback loop.[179] It should be noted that marriage of bimorphic soft actuators with additive manufacturing technologies could bring real breakthrough in the future development of artifical soft robots with bioinspired intelligence and more sophisticated capabilities.[180] Biohybrid artifical robots that combine living cells with bimorphic soft actuators could help reproduce similar organ or tissue construction and functions of organisms.[181] Through evolution and natural selection over billions of years, Nature has offered us unlimited precious gifts of soft actuation with extraordinary complexity and high efficiency such as birds

flying freely in the sky and fish swiming in the water. We should always remind us in our research that learning from mother nature could inspire and surprise us to answer fundamental questions in the development of truly intelligent soft actuators. It is anticipated that the united efforts and meaningful cooperation of engineers from different backgrounds and scientists from multidisciplinary fields in the future would give birth to multifunctional programmable and reconfigurable artifical soft robotics and machines that exhibit increased flexibility and adaptability as well as improved safety when working around humans.

Acknowledgements:

This work was financially supported by National Natural Science Foundation of China (No. 51973155), National Natural Science Funds for Distinguished Young Scholars (No. 51425306) and National Key R&D Program of China (No. 2016YFA0202302).

Received: ((will be filled in by the editorial staff))

Revised: ((will be filled in by the editorial staff))

Published online: ((will be filled in by the editorial staff))

References:

1. S. Kim, C. Laschi and B. Trimmer, *Trends Biotechnol.*, 2013, **31**, 287-294.
2. C. Majidi, *Adv. Mater. Technol*., 2019, **4**, 1800477.
3. S. M. Mirvakili and I. W. Hunter, *Adv. Mater.*, 2018, **30**, 1704407.33
4. S. I. Rich, R. J. Wood and C. Majidi, *Nat. Electron.*, 2018, **1**,102-112.
5. G. M. Whitesides, *Angew. Chem. Int. Ed.*, 2018, **57**, 2–18.
6. H. Zeng, P. Wasylczyk, D. S. Wiersma and A. Priimagi, *Adv. Mater.*, 2018, **30**, 1870174.
7. L. Hines, K. Petersen, G. Z. Lum and M. Sitti, *Adv. Mater.*, 2017, **29**, 1603483.
8. A. I. Egunov, J. G. Korvink and V. A. Luchnikov, *Soft Matter,* 2016, **12**, 45-52.
9. X. Wang, H. Huang, H. Liu, F Rehfeldt, X. Wang and K. Zhang, *Macromol. Chem. Phys.*, 2019, **220**, 1800562.
10. D. Niu, W Jiang, H. Liu, T. Zhao, B. Lei, Y. Li, L. Yin, Y. Shi, B. Chen and B. Lu, *Sic. Rep.*, 2016, **6**, 27366.
11. P. Rastogi, J. Njuguna and B. Kandasubramanian, *Eur. Polym. J.*, 2019, **121,** 109287.

12. A. Agrawal, T.H. Yun, S.L Pesek, W.G. Chapman and R. Verduzco, *Soft Matter*, 2014, **10**, 1411-1415.
13. X. Wang, Q. Liu, S. Wu, B. Xu and H. Xu, *Adv. Mater.*, 2019, **31**, 1807716.
14. H. Zeng, O. M. Wani, P. Wasylczyk, R. Kaczmarek and A. Priimagi, *Adv. Mater.*, 2017, **29**, 1701814.
15. S. Palagi, A.G. Mark, S.Y. Reigh, K. Melde, T. Qiu, H. Zeng, C. Parmeggiani, D. Martella, A. Sanchez-Castillo, N. Kapernaum, F. Giesselmann, D. S. Wiersma, E. Lauga and P. Fischer, *Nat. Mater.*, 2016, **15**, 647-653.
16. C Wang, K Sim, J Chen, H Kim, Z Rao, Y Li, W. Chen, J. Song, R. Verduzco and C. Yu, *Adv. Mater.*, 2018, **30**, 1706695.
17. W. Hu, G.Z. Lum, M. Mastrangeli and M Sitti, *Nature*, 2018, **554**, 81-85.
18. B. Shin, J. Ha, M. Lee, K. Park, G. H. Park, T. H. Choi, Kyu-Jin Cho and Ho-Young Kim, *Sci. Robot*, 2018, **3.**
19. S. A. Morin, R. F. Shepherd, S. W. Kwok, A. A. Stokes, A. Nemiroski and G. M. Whitesides, *Science*, 2012, **337**, 828-832.
20. E. W Hawkes, L. H. Blumenschein, J. D. Greer and A.M. Okamura, *Sci. Robot*, 2017, **2,** eaan3028.
21. M Wehner, R. L. Truby, D. J. Fitzgerald, B. Mosadegh, G. M. Whitesides, J. A. Lewis and R. J. Wood, *Nature*, 2016, **536**, 451–455.
22. T. Patino, R. Mestre and S. Sanchez, *Lab Chip*, 2016, **16**, 3626-3630.
23. A. H. Gelebart, D. J. Mulder, M. Varga, A. Konya, G. Vantomme, E. W. Meijer, R. L. B. Selinger and D. J. Broer, *Nature*, 2017, **546**, 632–636.
24. M. Amjadi and M. Sitti, *ACS Nano*, 2016, **10**, 10202–10210.
25. D. Gao, W. Ding, M. Nieto-Vesperinas, X. Ding, M. Rahman, T. Zhang, C. Lim and C. Qiu, *Light Sci. Appl.*, 2017, **6**, e17039.
26. X. Qian, Y. Zhao, Y. Alsaid, X. Wang, M. Hua, T. Galy, H. Gopalakrishna, Y. Yang, J. Cui, N. Liu, M. Marszewski, L. Pilon and X. He, *Nat. Nanotechnol.*, 2019, **14**, 1-8.
27. Y Yang, Y Tan, X Wang, W An, S Xu, W. Liao and Y. Wang, *ACS Appl. Mater. Interfaces*, 2018, **10**, 7688–7692.
28. J. Li, R. Zhang, L Mou, M. J. d. Andrade, X. Hu, K. Yu, J. Sun, T. Jia, Y. Dou, H. Chen, S. Fang, D. Qian and Z. Liu, *Adv. Funct. Mater.*,2019, **29**, 1808995.
29. T. van Manen, S. Janbaz and A. A. Zadpoor, *Mater. Today*, 2018, **21**, 144-163.
30. M. Kanik, S. Orguc, G. Varnavides, J. Kim, T. Benavides, D. Gonzalez, T. Akintilo, C. C. Tasan, A. P. Chandrakasan, Y. Fink and P. Anikeeva, *Science*, 2019, **365**, 145-150.

31. M. P. Cunha, Y. Foelen, T. A. P. Engels, K. Papamichou, M. Hagenbeek, M. G. Debije and A. P. H. J. Schenning, *Adv. Opt. Mater.*, 2019, **7**, 1801604.
32. L. Zhang, J. Pan, Y. Liu, Y. Xu and A. Zhang, *ACS Appl. Mater. Interfaces*, 2020, **12**, 6727–6735.
33. H. Ma, X. Zhang, R. Cui, F. Liu, M. Wang, C. Huang, J. Hou, G. Wang, Y. Wei, K. Jiang, L. Pan and K. Liu, *Nanoscale*, 2018, **10**, 11158-11164.
34. J. Deng, J. Li, P. Chen, X. Fang, X. Sun, Y. Jiang, W. Weng, B. Wang, and H. Peng, *J. Am. Chem. Soc.*, 2016, **138**, 225–230.
35. P. Cendula, S. Kiravittaya, Y. F. Mei, C. Deneke and O. G. Schmidt, *Phys. Rev. B*, 2009, **79**, 085429.
36. F. Ilievski, A. D. Mazzeo, R. F. Shepherd, X. Chen and G. M. Whitesides, *Angew. Chem.*, 2011, **50**, 1890-1895.
37. G. Liu, J. Kim, Y. Lu and L. P. Lee, *Nat. Mater.*, 2006, **5**, 27-32.
38. L. Chang, M. Huang, K. Qi, Z. Jing, L. Yang, P. Lu, Y. Hu and Y. Wu, *Macromol. Mater. Eng.*, 2019, **304**, 1800688.
39. Y. Naka, J. Mamiya, A. Shishido, M. Washio and T. Lkeda, *J. Mater. Chem.*, 2011, **21**, 1681-1683.
40. A. Kotikian, C. McMahan, E. C. Davidson, J. M. Muhammad, R.D. Weeks1, C. Daraio and J. A. Lewis, *Sci. Robot.*, 2019, **4**, 7044.
41. J. M. Boothby and T. H. Ware, *Soft Matter*, 2017, **13**, 4349-4356.
42. Z. Tian, B. Xu, B. Hsu, L. Stan, Z. Yang and Y. Mei, *Nano Lett.*, 2018, **18**, 3017-3023.
43. K. Liu, C. Cheng, J. Suh, R. T. ‐ Kong, D. Fu, S. Lee, J. Zhou, L. O. Chua and J. Wu, *Adv. Mater.*, 2014, **26**, 1746-1750.
44. S. Timoshenko, *Josa*, 1925, **11**, 233-255.
45. J. Chen, J. Feng, F. Yang, R. Aleisa, Q. Zhang and Y. Yin, *Angew. Chem.*, 2019, **131**, 9376-9382.
46. M. Weng, P. Zhou, L. Chen, L. Zhang, W. Zhang, Z. Huang, C. Liu and S. Fan, *Adv. Funct. Mater.*, 2016, **26**, 7244-7253.
47. L. Li, J. Meng, C. Hou, Q. Zhang, Y. Li, H. Yu and H. Wang, *ACS Appl. Mater. Interfaces*, 2018, **10**, 15122–15128.
48. M. Wang, Y. Han, L. Guo, B. Lin and H Yang, *Liq. Cryst.*, 2019, **46**, 1231-1240.
49. H. Liu, D. Niu, W. Jiang, T. Zhao, B. Lei, L. Yin, Y Shi, B. Chen and B. Lu, *Sens. Actuators A*, 2016, **239**, 45-53.
50. X. Wang, N. Jiao, S. Tung and L Liu, *ACS Appl. Mater. Interfaces*, 2019, **11**, 30290–30299.
51. Y. Yang, Y. Liu and Y. Shen, *Adv. Funct. Mater.*, 2020, **30**, 1910172.

52. Y. Wang, L. Zhang and P. Wang, *ACS Sustainable Chem. Eng.*, 2016, **4**, 1223–1230.
53. J. Zeng, D. Goldfeld and Y. Xia, *Angew. Chem.*, 2013, **125**, 4263-4267.
54. L. Zhou, Y. Tan, J. Wang, W. Xu, Y. Yuan, W. Cai, S. Zhu and J. Zhu, *Nat. Photonics*, 2016, **10**, 393–398.
55. B. Li, Q. Wang, R. Zou, X. Liu, K. Xu, W. Li and J. Hu, *Nanoscale*, 2014, **6**, 3274-3282.
56. M. Naguib, M. Kurtoglu, V. Presser, J. Lu, J. Niu, M. Heon, L. Hultman, Y. Gogotsi and M.W. Barsoum, *Adv. Mater.*, 2011, **23**, 4248-4253.
57. R. Li, L Zhang, L. Shi and P. Wang, *ACS Nano*, 2017, **11**, 3752-3759.
58. Z. Tang, Z. Gao, S. Jia, F. Wang and Y. Wang, *Adv. Sci.*, 2017, **4**, 1600437.
59. Y. Chen, Y. Zhao, S. J. Yoon, S. S. Gambhir and S. Emelianov, *Nat. Nanotechnol*, 2019, **14**, 465-472.
60. H. Jia, C. Fang, X. Zhu, Q. Ruan, Y. J. Wang and J. Wang, *Langmuir*, 2015, **31**, 7418–7426.
61. V. H. Nguyen, R. Tabassian, S. Oh, S. Nam, M. Mahato, P. Thangasamy, A. R. ‐ Abhari, W. ‐ J. Hwang, A. K. Taseer and Il ‐ K. Oh, *Adv. Funct. Mater.*, 2020, 1909504.
62. W. Cao, W. Feng, Y. Jiang, C. Ma, Z. Zhou, M. Ma, Y. Chen and F. Chen, *Mater. Horizons*, 2019, **6**, 1057-1065.
63. G. Cai, J. H. Ciou, Y. Liu, Y. Jiang and P. S. Lee, *Sci. adv.* 2019, **5**, eaaw7956.
64. M. Ji, N. Jiang, J. Chang and J. Sun, *Adv. Funct. Mater.*, 2014, **24**, 5412-5419.
65. L. Liu, M. Liu, L. Deng, B. Lin and H. Yang, *J. Am. Chem. Soc.*, 2017, **139**, 11333–11336.
66. Q. Tian, F. Jiang, R. Zou, Q. Liu, Z. Chen, M. Zhu, S. Yang, J. Wang, J. Wang and J. Hu, *ACS Nano*, 2011, **5**, 9761–9771.
67. H. Ren, M. Tang, B. Guan, K. Wang, J. Yang, F. Wang, M. Wang, J. Shan, Z. Chen, D. Wei, H. Peng and Z. Liu, *Adv. Mater.*, 2017, **29**, 1702590.
68. J. Wang, Y. Li, L. Deng, N. Wei, Y. Weng, S. Dong, D. Qi, J. Qiu and X. Chen, *Adv. Mater.*, 2017, **29**, 1603730.
69. H. Durr and H. B. Laurent, Ed., Elsevier Science Publishers B.V., Amsterdam, 1990.
70. L. L. Cabrera, V. Krongauz and H. Ringsdorf, *Angew. Chem. Int. Ed.*, 1987, **26**, 1178-1180.
71. L. D, Y. Feng, L. Wang and W. Feng, *Chem. Soc. Rev.*, 2018, **47**, 7339-7368.
72. X. Li, S. Ma, J. Hu, Y. Ni, Z. Lin and H. Yu, *J. Mater. Chem. C*, 2019, **7**, 622-629.
73. T. Ube, K. Kawasaki and T. Ikeda, *Adv. Mater.*, 2016, **37**, 8212-8217.
74. X. Lu, S. Guo, X. Tong, H. Xia and Y. Zhao, *Adv. Mater.*, 2017, **29**, 1606467.

75. W, Bao, F Miao, Z, Chen, H, Zhang, W, Jang, C. Dames and C. N. Lau, *Nat. Nanotechnol.*, 2009, **4**, 462-566.
76. S. Wang, Z. Liang, P. Gonnet, Y.-H. Liao, B. Wang, and C. Zhang, *Adv. Funct. Mater.*, 2007, **17**, 87-92.
77. W. Jiang, D. Niu, H. Liu, C. Wang, T. Zhao, L. Yin, Y. Shi, B. Chen, Y. Ding and B. Lu, *Adv. Funct. Mater*., 2014, **24**, 7598-7604.
78. Leeladhar and J. P. Singh, *ACS Appl. Mater. Interfaces*. 2018, **10**, 33956–33965.
79. H. Lim, T. Park, J. Na, C. Park, B. Kim and E. Kim, *Npg Asia Mater.*, 2017, **9**, e399.
80. A. E Aliev, J. Oh, M. E. Kozlov, A. A. Kuznetsov, S. Fang, A. F. Fonseca, R. Ovalle and M. Zhang, *Science*, 2009, **323**, 1575-1578.
81. H. Deng, C. Zhang, J. W Su, Y. Xie, C. Zhang and J. Lin, *J. Mater. Chem. B*, 2018, **34**, 5415-5423.
82. Y. Maniwa, R. Fujiwara, H. Kira, H. Tou, H. Kataura, S. Suzuki, Y. Achiba, E. Nishibori, M. Takata, M. Sakata, A. Fujiwara and H. Suematsu, *Phys. Rev. B*. 2001. **64**. 241402.
83. W. Bao, F. Miao, Z. Chen, H. Zhang, W. Jang, W Jang, C. Dames and C. N. Lau, *Nat. Nanotechnol.*, 2009, **4**, 562-566.
84. O. Sul, S. Jang and E.-H. Yang, *IEEE Trans. Nanotechnol*., 2010, **10**, 985-990.
85. Y. Kuru, M. Wohlschlögel, U. Welzel and E. J. Mittemeijer, *Surf. Coat. Tech.*, 2008, **202**, 2306-2309.
86. Y. Tai, G. Lubineau and Z. Yang, *Adv. Mater.*, 2016, **28**, 4660-4670.
87. L. Yang, L. Chang, Y. Hu, M. Huang, Q. Ji, P. Lu, J. Liu, W. Chen and Y. Wu, *Adv. Funct. Mater.*, 2020, **30**, 1908842.
88. X. Wang, K. H. Chan, Y. Cheng, T. Ding, T. Li, S. Achavananthadith, S. Ahmet, J. S. Ho, G. W. Ho, *Adv. Mater.*, 2020, **32**, 2000351.
89. X. Zhang, Z. Yu, C. Wang, D. Zarrouk, J.-W. T Seo, J. C. Cheng, A. D. Buchan, K. Takei, Y. Zhao, J. W. Ager, J. Zhang, M. Hettick, M. C. Hersam, A. P. Pisano, R. S. Fearing and A. Javey, *Nat. Commun.*, 2014, **5**, 1-8.
90. Y. Hu, J. Liu, L. Chang, L. Yang, A. Xu, K. Qi, P. Lu, G. Wu, W. Chen and Y. Wu, *Adv. Funct. Mater.*, 2017. **27**. 1704388.
91. B. Han, Y. Zhang, L. Zhu, Y. Li, Z. Ma, Y. Liu, X. Zhang, X. Cao, Q. Chen, C. Qiu and H. Sun, *Adv. Mater.*, 2019. **31**. 1806386.
92. Y. Hu, G. Wu, T. Lan, J. Zhao, Y. Liu and W. Chen, *Adv. Mater.*, 2015. **27**. 7867-7873.
93. M. Kauranen and A. V. Zayats, *Nat. Photonics*, 2012, **6**, 737-748.
94. C. M. Kolodziej and H. D. Maynard, *J. Am. Chem. Soc.* 2012, **134**, 12386–12389.
95. L. Xia, R. Xie, X. Ju, W. Wang, Q. Chen and L. Chu, *Nat. Commun.*, 2013, **4**, 1-11.

96. D. L. Thomsen, P. Keller, J. Naciri, R. Pink, H. Jeon, D. Shenoy and B. R. Ratna, *Macromolecules*, 2001, **34**, 5868–5875.
97. A. Buchsteiner, A. Lerf and J. Pieper, *J. Phys. Chem. B*, 2006, **110**, 22328–22338.
98. J. Zhu, C. M. Andres, J. Xu, A. Ramamoorthy, T. Tsotsis and N. A. Kotov, *ACS Nano*, 2012, **6**, 8357–8365.
99. Y. Dong, J. Wang, X. Guo, S. Yang, M. O. Ozen, P. Chen, X. Liu, W.i Du, F. Xiao, U. Demirci and B. Liu, *Nat. Commun.*, 2019, **10**, 1-10.
100. Y. Zhang, J. Ma, S. Liu, D. Han, Y. Liu, Z. Chen, J. Mao and H. Sun, *Nano Energy*, 2020, **68**, 104302.
101. W. Wang, C. Xiang, Q. Zhu, W. Zhong, M. Li, M. Li, K. Yan, and D. Wang, *ACS Appl. Mater. Interfaces*, 2018, **10**, 27215–27223.
102. D. Gao, M. Lin, J. Xiong, S. Li, S. N. Lou, Y. Liu, J. Ciou, X. Zhou and P. S. Lee, *Nanoscale Horiz.*, 2020, **5**, 730-738.
103. H. Li and J. Wang, *ACS Appl. Mater. Interfaces*, 2019, **11**, 10218–10225.
104. Y. Hu, K. Qi, L. Chang, J. Liu, L. Yang, M. Huang, G. Wu, P. Lu, W. Chen and Y. Wu, *J. Mater. Mater. C*, 2019, **7**, 6879-6888.
105. Y. Tu, J. Yuan, D. Lei, H. Tan, J. Wei, W. Huang and L. Zhang, *J. Mater. Mater. A*, 2018, **6**, 8238-8243.
106. L. Zhang, X. Qiu, Y. Yuan and T. Zhang, *ACS Appl. Mater. Interfaces*, 2017, **9**, 41599-41606.
107. J. Wu, Q. Gu, B. S. Guiton, N. P. D. Leon, L. Ouyang and H. Park, *Nano Lett.*, 2006, **6**, 2313–2317.
108. J. Cao, E. Ertekin, V. Srinivasan, W. Fan, S. Huang, H. Zheng, J. W. L. Yim, D. R. Khanal, D. F. Ogletree, J. C. Grossman and J. Wu, *Nat. Nanotechnol.*, 2009, **4**, 732-737.
109. K. Liu, C. Cheng, Z. Cheng, K. Wang, R. Ramesh and J. Wu, *Nano Lett.*, 2012, 12, 6302–6308.
110. K. Wang, C. Cheng, E. Cardona, J. Guan, K. Liu and J. Wu, *ACS Nano*. 2013, **7**, 2266–2272.
111. R. Cabrera, E. Merced, N. Sepúlveda and F.E. Fernández, *J. Appl. Phys.*, 2011, **110**, 094510.
112. Y. Zhao, J. Hwan Lee, Y. Zhu, M. Nazari, C. Chen., H. Wang, A. Bernussi1, M. Holtz, and Z. Fan, *J. Appl. Phys.*, 2012, **111**, 053533.
113. N. R. Mlyuka, G. A. Niklasson and C. G. Granqvist, *Appl. Phys. Lett.*, 2009, **95**, 171909.
114. T. Wang, D. Torres, F. E. Fernández, C. Wang and N. Sepúlveda, *Sci. Adv.*, 2009, **95**, 171909.

115. T. Wang, D. Torres, F. E. Fernández, A. J. Green, C. Wang and N. Sepúlveda, *ACS Nano*, 2015, **9**, 4371–4378.
116. H. Ma, J. Hou, X. Wang, J. Zhang, Z. Yuan, L. Xiao, Y. Wei, S. Fan, K. Jiang and Kai Liu, *Nano Lett.*, 2017, **17**, 421–428.
117. P. Chen, R. Shi, N. Shen, Z. Zhang, Y. Liang, T. Li, J. Wang, D. Kong, Y. Gan, A. Amini, N. Wang and C. Cheng, *Adv. Intell. Syst.*, 2000051.
118. M. K. Jaiswal, R. Banerjee, P. Pradhan and D. Bahadura, *Colloids Surf. B*, 2010, **81**, 185-194.
119. J. Mu, C. Hou, B. Zhu, H. Wang, Y. Li and Q Zhang, *Sci. Rep.*, 2015, **5**, 1-7.
120. D. Kim, H. S. Lee and J. Yoon, *Sci. Rep.*, 2016, **6**, 1-10.
121. J. N. Tiwari, K. Mahesh, N. H. Le, K. C. Kemp, R. Timilsina, R. N. Tiwari and K. S. Kim, *Carbon*, 2013, **56**, 173-182.
122. Q. Shi, H. Xia, P. Li, Y. Wang, L Wang, S. Li, G. Wang, C. Lv, L. Niu and H. Sun, *Adv. Opt. Mater.*, 2017, **5**, 1700442.
123. Z. Chen, R. Cao, S. Ye, Y. Ge, Y. Tu and X. Yang, *Sensor. Actuat. B Chem.*, 2018, **255**, 2971-2978.
124. J.-H. Na, A. A. Evans, J. Bae, M. C. Chiappelli, C. D. Santangelo, R. J. Lang, T, C. Hull and R, C. Hayward, *Adv. Mater.*, 2015, **27**, 79-85.
125. J. L. Silverberg, J.-H. Na, A. A. Evans, B. Liu, T. C. Hull, C. D. Santangelo, R. J. Lang, R.C. Hayward and I. Cohen, *Nat. Mater.*, 2015, **14**, 389-393.
126. Z. Zhu, E. Senses, P. Akcora, S. A. Sukhishvili, *Acs Nano*, 2012, **6**, 3152-316.
127. E. Wang, M. S. Desai and S-W Lee, *Nano Lett.*, 2013, **13**, 2826–2830.
128. E. Lee, D. Kim, H. Kim and J Yoon, *Sci. Rep.*, 2015, **5**, 15124.
129. S. Zhang, L. Chu, D. Xu, J. Zhang, X. Ju and R. Xie, *Polym. Advan. Technol.*, 2008, 19, 937-943.
130. E. Lee, H. Lee, S. I. Yoo and J. Yoon, *ACS Appl. Mater. Interfaces*, 2014, **6**, 16949–16955.
131. P. Fan, Z. Fan, F. Huang, J. Yang, F. Chen, Z. Fei and M. Zhong, *Ind. Eng. Chem. Res*., 2019, **58**, 3893–390.
132. E. Zhang, T. Wang, W. Hong, W. Sun, X. Liu and Z. Tong, *J. Mater. Chem. A*, 2014, **2**, 15633-15639.
133. Q. Zhao, Y. Liang, L. Ren, Z. Yu, Z. Zhang, F. Qiu and L. Ren, *J. Mater. Chem. B*, 2016, **6**, 1260-1271.
134. M. Moua, R. R. Kohlmeyer and J. Chen, *Angew. Chem.*, 2013, **52**, 9234-9237.
135. J. Naciri, A. Srinivasan, H. Jeon, N. Nikolov, P. Keller and B. R. Ratna, *Macromolecules*, 2003, **36**, 8499–8505.

136. H. Yang, A. Buguin, J.-M. Taulemesse, K. Kaneko, S. Méry, A. Bergeret and P. Keller, *J. Am. Chem. Soc.*, 2009, **131**, 15000–15004.
137. Y. Ji, Y. Y. Huang, R. Rungsawan and E. M. Terentjev, *Adv. Mater.*, 2010, **22**, 3436-3440.
138. J. E. Marshall, Y. Ji, N. Torras, K. Zinoviev and E. M. Terentjev, *Soft Matter*, 2012, **8**, 1570-1574.
139. L. Yang, K. Setyowati, A. Li, S. Gong and J. Chen, *Adv. Mater.*, 2008, **20**, 2271-2275.
140. S. Banisadr and J. Chen, *Sci. Rep.*, 2017, **7**, 1-9.
141. X. Fan, B. C. King, J. Loomis, E. M. Campo, J. Hegseth, R. W Cohn, E. Terentjev and B. Panchapakesan, *Nanotechnology*, 2014, **25**, 355501.
142. L. Yu, Z. Cheng, Z. Dong, Y. Zhang and H. Yu, *J. Mater. Chem. C*, 2014, **2**, 8501-8506.
143. Z. Cheng, T. Wang, X. Li, Y. Zhang and H. Yu, *ACS Appl. Mater. Interfaces*, 2015, **7**, 27494–27501.
144. H. Yang, J. Liu, Z. Wang, L. Guo, P. Keller, B. Lin, Y. Sun and X. Zhang, *Chem. Commun.*, 2015, **51**, 12126-12129.
145. A. W. Hauser, D. Liu, K. C. Bryson, R. C. Hayward and D. J. Broer, *Macromolecules*, 2016, **49**, 1575–1581.
146. L. Dong and Y. Zhao, *Mater. Chem. Front.*, 2018, **2**, 1932-1943.
147. H. Tian, Z. Wang, Y. Chen, J. Shao, T. Gao and S. Cai, *ACS Appl. Mater. Interfaces*, 2018, **10**, 8307–8316.
148. R. Lan, J. Sun, C. Shen, R. Huang, Z. Zhang, L. Wang and H. Yang, *Adv. Mater.*, 2020, **32**, 1906319.
149. L. Dong, X. Tong, H. Zhang, M. Chen and Y. Zhao, *Mater. Chem. Front.*, 2018, **2**, 1383-1388.
150. B. Zuo, M. Wang, B. Lin and H. Yang, *Nat. Commun.*, 2019, **10**, 1-11.
151. A. Schwartz and D. Koller, *Plant Physiol.*, 1978, **61**, 924-928.
152. M. P. M. Dicker, J. M. Rossiter, I. P. Bon and P. M. Weaver, *Bioinspir. Biomim.*, 2014, **9**, 036015.
153. F. Lancia, A. Ryabchun and N. Katsonis, *Nat. Rev. Chem.*, 2019, **3**, 536-551.
154. C. Li, A. Iscen, H. Sai, K. Sato, N. A. Sather, S. M. Chin, Z. Álvarez, L. C. Palmer, G. C. Schatz and S. I. Stupp, *Nat. Mater.*, 2020, **19**, 900-909.
155. J. Mamiya, A. Kuriyama, N. Yokota, M. Yamada and T. Ikeda, *Chem.-Eur. J.*, 2015, **21**, 3174-3177.
156. H. Yu and T. Ikeda, *Adv. Mater.*, 2011, **23**, 2149-2180.
157. T. J. White and D. J. Broer, *Nat. Mater.*, 2015, **14**, 1087-1098.

158. F. Weigert, *Verh. Dtsch. Phys. Ges.*, 1919, **21**, 479-491.
159. W. Wu, J. Yang, J. Hua, J. Tang, L. Zhang, Y. Long and H. Tian, *J. Mater. Chem.*, 2010, **20**, 1772-1779.
160. P. Weis, W. Tian and S. Wu, *Chem.-Eur. J.*, 2018, **24**, 6494-6505.
161. X. Pang, J. Lv, C. Zhu, L. Qin and Y. Yu, *Adv. Mater.*, 2019, **31**, 1904224.
162. M. Yamada, M. Kondo, J. Mamiya, Y. Yu, M. Kinoshita, C. J. Barrett, T. Ikeda, *Angew. Chem.*, 2008, **47**, 4986-4988.
163. R. Tang, Z. Liu, D. Xu, J. Liu, L. Yu and H. Yu, *ACS Appl. Mater. Interfaces*, 2015, **7**, 8393–8397.
164. Z. Cheng, S. Ma, Y. Zhang, S. Huang, Y. Chen and H. Yu, *Macromolecules*, 2017, **50**, 8317–8324.
165. D. E. Hagaman, S. Leist, J. Zhou and H. Ji, *ACS Appl. Mater. Interfaces*, 2018, **10**, 27308–27315.
166. S. Ma, X. Li, S. Huang, J. Hu and H. Yu, *Angew. Chem.*, 2019, **131**, 2681-2685.
167. J. Hu, X. Li, Y. Ni, S. Ma and H. Yu, *J. Mater. Chem. C*, 2018, **6**, 10815-10821.
168. Z. Jiang, Y. Xiao, L. Yin, L. Han and Y. Zhao, *Angew. Chem.*, 2020, **132**, 4955-4961.
169. R. C. P. Verpaalen, M. P. Cunha, T. A. P. Engels, M. G. Debije and A. P. H. J. Schenning, *Angew. Chem. Int. Edit.*, 2020, **59**, 4532-4536.
170. Z. Jiang, M. Xu, F. Li and Y. Yu, *J. Am. Chem. Soc.*, 2013, 135, 16446–16453.
171. H. Zeng, M. Lahikainen, O.M. Wani, A, Berdin and A. Priimagi, *Nat. Commun.*, 2019, **10**, 1-9.
172. J. Li, X. Zhou and Z. Liu, *Adv. Opt. Mater.*, 2020, 2000886.
173. L. Zhou, Q. Liu, X. Lv, L. Gao, S. Fang and H. Yu, *J. Mater. Chem. C*, 2016, **4**, 9993-9997.
174. X. Lu, H. Zhang, G. Fei, B. Yu, X. Tong, H. Xia and Y. Zhao, *Adv. Mater.*, 2018, **30**, 1706597.
175. M. Wang, B. Lin and H. Yang, *Nat. Commun.*, 2016, **7**, 1-8.
176. S. A. Morin, R. F. Shepherd, S. W. Kwok, A. A. Stokes, A. Nemiroski and G. M. Whitesides, *Science*, 2012, **337**, 828-832.
177. S. Mao, J. Chang, H. Pu, G. Lu, Q. He, H. Zhang and J. Chen, *Chem. Soc. Rev.*, 2017, **46**, 6872-6904.
178. F. Shahzad, M. Alhabeb, C. B. Hatter, B. Anasori, S. M. Hong, C. M. Koo and Y. Gogotsi, *Science*, 2016, **353**. 1137-1140.

179. J. Yang, J. Mun, S. Y. Kwon, S. Park, Z. Bao and S. Park, *Adv. Mater.*, 2019, **31**, 1904765.
180. T. J. Wallin, J. Pikul and R. F. Shepherd, *Nat. Rev. Mater.*, 2018, **3**, 84-100.
181. L. Sun, Y. Yu, Z. Chen, F. Bian, F. Ye, L. Sun and Y. Zhao, *Chem. Soc. Rev.*, 2020.